CHARACTERISTICS OF AN AIRFOIL EXTENDING THROUGH A CIRCULAR JET

Thesis by

Scott C. Rethorst

In Partial Fulfillment of the Requirements

for the Degree of

Doctor of Philosophy

California Institute of Technology

Pasadena, California

1956

TO

JOHN AND SUSAN

ACKNOWLEDGEMENT

The author wishes to express his deep appreciation to Dr. Homer J. Stewart for his help and encouragement in carrying out this research. His interest, as well as the guidance of Dr. Clark B. Millikan and Dr. Morgan Ward, were a constant source of inspiration.

Thanks are also due to Mr. Kenneth Ralston of the Institute of Numerical Analysis at UCLA and to Dr. Dick Talmadge of the Lockheed Aircraft Corporation for their help in programming and carrying out the numerical computations by electronic data processing equipment.

In addition he would like to thank Mrs. Betty Wood and Mrs. Elizabeth Fox for their assistance in preparing the manuscript.

ABSTRACT

A method has been derived for the determination of the downwash in the field of an airfoil extending through a circular jet. This solution has been applied particularly to the region aft of the lifting line in the plane of the airfoil, to determine the lift distribution on a wing extending through a circular jet.

The method of solution is essentially based on a division of the flow induced by the jet boundary into parts which are even and odd with respect to the direction of flow. The analysis due to the even part alone is similar to previous theories, which in effect disregarded the odd part. Such previous results based on the even part alone differ considerably from the experimental values. The results based on the total of the even and odd parts show good agreement with the experiments, illustrating the necessity of including the odd part of the flow when the segment of the wing immersed in the jet is of low aspect ratio.

The problem has been solved in parametric form, so that the results may be employed to determine the characteristics of any geometry wing-jet combination at any jet velocity ratio.

TABLE OF CONTENTS

TABLE OF CONTENTS (Cont'd)

LIST OF FIGURES

LIST OF TABLES

I. INTRODUCTION

The problem of determining the characteristics of an airfoil extending through a circular jet has been investigated from several points of view. One is the influence of a propeller slipstream on an airplane's flight characteristics. Another is the influence of the boundaries of a wind tunnel on an airfoil being tested therein.

An analytical treatment of the problem of a wing in a propeller slipstream was given by Koning (Ref. 1), based on lifting line theory. The results of Koning's analysis, because of his method of computation, are valid only for small increments of the jet velocity. Other early estimates (Refs. 2, 3, 4) were based on semi-empirical factors, and gave satisfactory results within the speed-power range for which they were developed. However, the higher ratios of jet velocities attainable through turbo-prop engines have stimulated renewed interest in solutions valid at all jet velocities. This interest is further augmented by the development of certain types of vertical take-off aircraft, and other configurations where the higher jet velocities now attainable produce a first order effect on performance.

Graham, Lagerstrom, Licher, and Beane of the Douglas Aircraft Company (Ref. 5) recently surveyed the slipstream problem, and extended Koning's results in a form valid (within the original assumptions) at all jet velocities. Graham's study also included an application of slender body theory to this problem. These two theories were compared with the experimental data of Stuper (Ref. 6), which seemed to lie between the two theories.

In most cases of interest the width of a propeller slipstream is of the same order as the wing chord immersed in it. With the aspect ratio of the immersed segment thus of the order of one, it would seem lifting surface theory would be required to properly describe the actual conditions. The finding of Graham that the available experimental data lay midway between the two limiting theories, lifting line and slender body, would appear to support this view.

The difficulty in applying lifting surface theory to this problem is the determination of the downwash due to the boundary of the jet at points downstream of the lifting line. However, the downwash aft of the lifting line is of interest in certain wind-tunnel problems, and has been determined by Lotz (Ref. 7) and Burgers (Ref. 8). These wind-tunnel investigations were situations where the outer velocity was zero and the airfoil lay entirely within the jet, and as such were special cases of the general problem of an airfoil extending through a circular jet. A similar investigation for a closed wind tunnel was carried out by Eisenstadt (Ref. 9).

This thesis develops the general case where there exists an outer velocity and where the airfoil extends through the jet. This permits the calculation of the downwash due to the boundary in the entire field aft of the lifting line. Any wing problem in principle can then be solved by lifting surface methods.

As an example, a wing problem is solved by finite step methods (Ref. 10), based on the approximate lifting surface method of Weissinger (Ref. 11).

II. NOTATION

r_o	Jet radius
x, y, z	Rectangular coordinates (Fig. 1)
ξ, η, ζ	Non-dimensionalized rectangular coordinates, $\frac{x}{r_o}, \frac{y}{r_o}, \frac{z}{r_o}$
$\bar{x}, \bar{y}, \bar{z}$	Rectangular coordinate running variables
α, β, γ	Non-dimensionalized rectangular coordinate running variables, $\frac{\bar{x}}{r_o}, \frac{\bar{y}}{r_o}, \frac{\bar{z}}{r_o}$
x, r, θ	Cylindrical coordinates
ρ	Non-dimensionalized radius, $\frac{r}{r_o}$
s	Semi-width of horseshoe vortex
b	Wing span
S	Wing area
$\underline{A}$	Vector velocity potential of flow induced by horseshoe vortex
ϕ	Scalar velocity potential of flow induced by jet boundary
V_j	Jet velocity
V_o	Outer or free stream velocity
μ	V_o/V_j
Γ	Circulation strength
$\underline{v}$	Vector perturbation velocity
u, v, w	Rectangular perturbation velocities
u_r	Radial perturbation velocity
I, K	Modified Bessel functions
A, B	Coefficients in series representation of ϕ
p	Summation index

λ	Variable of integration
c, d	Spanwise locations of horseshoe vortices, non-dimensionalized with respect to jet radius r_o
h	Perpendicular distance to a line vortex
R'	Three-dimensional non-dimensionalized potential distance = $\sqrt{\xi^2 + (\eta-\beta)^2 + \zeta^2}$
R	Two-dimensional non-dimensionalized potential distance = $\sqrt{(\eta-\beta)^2 + \zeta^2}$
J	Integral defined in text
n	Number designating a particular horseshoe vortex, starting from left wing tip
ν	Number designating a particular downwash point, starting from left wing tip
$d\underline{\ell}$	Differential length element of horseshoe vortex, non-dimensionalized with respect to jet radius r_o
q	Variable defined in text: $q = \lambda\xi$
δ	Complex variable = $\eta + i\zeta = \rho e^{i\theta}$
P_ν	Downwash points
Q_ν	Vortex points
N	Number of horseshoe vortices across total wing span
$F(\tilde{x}, \tilde{y})$	Downwash velocity at any point $(\tilde{x}, \tilde{y})$ caused by a rectangular horseshoe vortex of unit semi-width and circulation strength equal to 4π
$F_{\nu n}$	Wing downwash coefficient; the downwash at any downwash point P_ν due to the nth horseshoe vortex

$G(\xi, \eta)$ Downwash velocity at any point (ξ, η) caused by a rectangular horseshoe vortex of unit semi-width and circulation strength equal to 4π

$G_{\nu n}$ Boundary downwash coefficient; the downwash at any point P_ν due to the nth horseshoe vortex

p, q Coordinates of a point on the wing surface with respect to root quarter chord, based on semi-width of horseshoe vortex

$\tilde{x}, \tilde{y}$ Coordinates of a point in the wing surface with respect to the origin of a unit horseshoe vortex, based on semi-width of horseshoe vortex

W Wronskian of Bessel functions $= I(\lambda)K'(\lambda) - I'(\lambda)K(\lambda) = -\frac{1}{\lambda}$

$\overline{W}$ Modified Wronskian $= V_o^2 I'(\lambda) K(\lambda) - V_j^2 I(\lambda) K'(\lambda)$

Note $\lim_{V_o \to V_j} \overline{W} = +\frac{1}{\lambda} V_j^2$

III. ANALYSIS OF DOWNWASH DUE TO THE JET BOUNDARY

The problem, as illustrated in Figure 2, is an airfoil spanning a circular jet. This circular jet of velocity V_j is bounded by an infinite outer flow of velocity V_o . The finite wing extends symmetrically completely across the jet into the outer flow on both sides.

In the analysis, the airfoil will be replaced by a series of finite horseshoe vortices. The case for such a vortex inside or outside of the jet will then be solved separately. These horseshoe vortices, illustrated in Figure 3, will be represented in width parametrically, so that combinations may later be superimposed to represent any arbitrary jet wing combination. The circulation around the horseshoe vortex as illustrated is taken as positive.

The fluid is assumed to be an ideal, incompressible, nonviscous fluid, and this leads to the Laplace equation as the governing equation.

The boundary of the jet is a free surface. The presence of different velocities on its two sides gives rise to a vortex sheet on the boundary. This vortex sheet has associated with it a flow system such that the required conditions on pressure and continuity of the boundary are satisfied.

Thus the requirements of the jet boundary determine the flow, aside from the singularities represented by the wing and its wake. Two conditions must be satisfied on the boundary. In a linearized small perturbation theory, these are: First, the pressure of the inside flow (region j) must at the boundary equal the

pressure of the outside flow (region o). Otherwise, the acceleration of the fluid would be infinite across the boundary. In terms of the perturbation velocity, $\underline{v}$, whose axial and radial components are u and u_r respectively, this condition is written:

$$V_j u_j = V_o u_o \tag{1}$$

The second boundary condition is one of continuity, and states that the boundary must consist of streamlines, that is, the inside and outside flow must be tangent at the boundary. For a circular jet, this tangency condition is expressed as:

$$V_o u_{r_j} = V_j u_{r_o} \tag{2}$$

The perturbation flow $\underline{v}$ is composed of two parts, that due to the wing and that due to the boundary. The flow due to the wing, or due to system of horseshoe vortices used to represent it, may be readily determined by the Biot Savart law. The essential problem then is to determine the flow due to the jet boundary. The sum of the two flows then constitutes the total perturbation flow.

We note the single elementary horseshoe vortex of strength Γ may be decomposed into two halves, one even (1) and one odd (2), each of strength $\frac{\Gamma}{2}$, as illustrated in Figure 4. These two systems are independent, and satisfy the boundary conditions independently.

This decomposition of the vortex into its even and odd parts with respect to x will facilitate the solution of the problem, as the even part is two-dimensional, and may be readily solved by two-

dimensional potential theory. The solution of the odd part, while more complicated, may be facilitated by employing antisymmetry conditions.

A. Horseshoe Vortex Inside Jet

The elementary horseshoe vortex inside the jet is first decomposed into its even and odd parts. Each of these halves satisfies the boundary conditions separately, so we may adopt whatever method of solution is most feasible for each case.

1. Even System

The even system, as illustrated in Figure 4, is two-dimensional. This place flow may then be solved most simply by two-dimensional potential theory. In terms of our boundary conditions, the condition (1) has vanished with the x component of the perturbation velocity. However, the radial boundary condition (2) still applies.

This requirement, for the case of a vortex located inside the jet, may be met by an image system consisting of vortices located outside the jet at the inverse points, as shown in Figure 5.

It has been shown (Ref. 1, p. 391) that, when a real vortex is located inside a jet, the contribution to the motion inside the jet due to the boundary, is that represented by this fictitious image system outside the boundary, modified in intensity by the factor $+\frac{V_j^2 - V_o^2}{V_j^2 + V_o^2}$. Thus when the outer velocity V_o is zero, the image strength is undiminished. As V_o approaches V_j, the image strength vanishes with the boundary.

Also, the contribution of the boundary to the motion outside the jet, due to a real vortex located inside the jet, in the presence of a boundary, is that of the real vortex itself, modified in intensity by the factor $-\frac{(V_j-V_o)^2}{V_j^2+V_o^2}$. When the outer velocity V_o is zero, this boundary contribution is undiminished, and completely cancels the real vortex inside. As the outer velocity V_o approaches V_j, the boundary vanishes, and the effect of the real vortex inside is undiminished.

a. Effect Inside Jet

For a real horseshoe vortex of strength Γ lying in the plane $z=0$, of small but finite span extending between two parametric non-dimensionalized points c and d, the even part consists of two line vortices of strength $\Gamma/2$ extending to $\pm\infty$ through these points. The image line vortices then extend through the inverse points of c and d, namely $\frac{1}{c}$ and $\frac{1}{d}$ respectively.

Since the image system replaces the boundary, the downwash due to the boundary, for the even system, may be obtained as the downwash due to the image system. This may be obtained by a straightforward application of the Biot Savart law.

For two line vortices through points c and d, as illustrated in Figure 5, the downwash induced at any point in the jet η, in the plane of the vortex due to the image vortices, may be found as follows:

For a doubly infinite vortex of strength $\Gamma/2$ the induced downwash is:

$$w(\eta) = \frac{\Gamma/2}{2\pi h}$$

where h is the perpendicular distance from the point η to the vortex. Hence for the image pair located at the inverse points of c and d, where the first subscript on $w(\eta)$ refers to the location of the effect point; the second to the location of the real vortex;

$$w_{jj}(\eta) = \frac{\Gamma}{4\pi r_o}\left[\frac{1}{\frac{1}{d} - \eta} - \frac{1}{\frac{1}{c} - \eta}\right]$$

and for the image pair located at the inverse points of -c and -d:

$$w_{jj}(\eta) = \frac{\Gamma}{4\pi r_o}\left[\frac{1}{\frac{1}{d} + \eta} - \frac{1}{\frac{1}{c} + \eta}\right]$$

Hence for a pair of finite horseshoe vortices, symmetrically spaced with respect to the axis of the jet, the downwash due to the image of the even part, induced at a point η inside the jet, taking into account the image strength factor, is:

$$w_{jj}(\eta) = \frac{V_j^2 - V_o^2}{V_j^2 + V_o^2} \frac{\Gamma}{4\pi r_o}\left[\frac{1}{\frac{1}{d} - \eta} - \frac{1}{\frac{1}{c} - \eta} + \frac{1}{\frac{1}{d} + \eta} - \frac{1}{\frac{1}{c} + \eta}\right] \tag{3}$$

b. Effect Outside Jet

Here the downwash induced at a point η outside the jet by the boundary due to a pair of real line vortices of strength $\Gamma/2$ extending to $\pm\infty$ through points c and d is:

$$w_{oj}(\eta) = \frac{\Gamma}{4\pi r_o}\left[\frac{1}{\eta - c} - \frac{1}{\eta - d}\right]$$

and that induced by the vortex pair at -c and -d is:

$$w_{oj}(\eta) = \frac{\Gamma}{4\pi r_o} \left[\frac{1}{\eta + d} - \frac{1}{\eta + c} \right]$$

Hence for a pair of finite horseshoe vortices, symmetrically spaced with respect to the axis of the jet, the downwash induced by the boundary, due to the even part, at a point η outside the jet, taking into account the image strength factor, is:

$$w_{oj}(\eta) = - \frac{(V_j - V_o)^2}{V_j^2 + V_o^2} \frac{\Gamma}{4\pi r_o} \left[\frac{1}{\eta - c} - \frac{1}{\eta - d} + \frac{1}{\eta + d} - \frac{1}{\eta + c} \right] \qquad (4)$$

2. Odd System

An elementary horseshoe vortex inside the jet will induce a velocity perturbation, the vector potential of which in a uniform flow we represent by $\underline{A}$. In addition, the requirements of the boundary induce a further flow, the potential of which we represent by ϕ.

The total perturbation velocity $\underline{v}$ for the odd system (2) of Figure 4 is thus the sum:

$$\underline{v} = \nabla \times \underline{A} + \nabla \phi \qquad (5)$$

The part of the perturbation velocity due to the horseshoe vortex itself, $\underline{v_A}$ represented by the vector potential $\underline{A}$, is known. The part due to the boundary, $\underline{v_\phi}$, represented by the potential ϕ, is unknown. However, the total perturbation velocity $\underline{v}$ must satisfy the boundary conditions (1) and (2). Hence we may

use these boundary conditions to find the unknown potential ϕ , and from this potential ϕ we may then find the boundary induced downwash for the odd system.

We may represent the potential ϕ conveniently by a series of the form for $\rho<1$

$$\phi_j = \frac{2\Gamma}{\pi^2} \sum_{p=o}^{\infty} \sin(2p+1)\theta \int_o^{\infty} A_{2p+1}(\lambda) I_{2p+1}(\lambda\rho) \sin \xi\lambda d\lambda \tag{6}$$

and for $\rho > 1$

$$\phi_o = \frac{2\Gamma}{\pi^2} \sum_{p=o}^{\infty} \sin(2p+1)\theta \int_o^{\infty} B_{2p+1}(\lambda) K_{2p+1}(\lambda\rho) \sin \xi\lambda d\lambda \tag{7}$$

The potential ϕ is anti-symmetric with respect to the xy plane, since the downwash $w = \frac{\partial\phi}{\partial z}$ is symmetric with respect to this plane. Hence for the potential we use only a sine θ series. Also we use only the odd θ terms as the even θ terms are anti-symmetric with regard to the z plane, whereas the flow is symmetric about this plane.

Also from Figure 4, the downwash w in the odd system (2) is seen to be odd with respect to x . Hence ϕ is also odd in x . We may thus represent ϕ by a sine series in x , or in ξ in non-dimensionalized form.

With this form of the potential ϕ established, we must find the unknown coefficients $A(\lambda)$ and $B(\lambda)$, employing the known velocity due to the vector potential $\underline{A}$ of the horseshoe vortex itself.

The relation between the vector potential $\underline{A}$ and its resulting velocity field $\underline{v_A}$ is:

$$\underline{v_A} = \nabla \times \underline{A} = \begin{vmatrix} \underline{i} & \underline{j} & \underline{k} \\ \frac{\partial}{\partial x} & \frac{\partial}{\partial y} & \frac{\partial}{\partial z} \\ A_x & A_y & A_z \end{vmatrix} \tag{8}$$

where A_x, A_y, A_z are the rectangular components of the vector potential $\underline{A}$. For a rectangular horseshoe vortex lying in the plane $z = o$ as illustrated in Figure 4, the potential of the bound vortex is A_y and the potential of the trailing vortex is A_x.

For the bound vortex $A_x = A_z = 0$, and

$$u_{A_{bd}} = \underline{i} \cdot \underline{v_A} = -\frac{\partial A_y}{\partial z} = -\frac{\partial A_y}{\partial r}\frac{\partial r}{\partial z} - \frac{\partial A_y}{\partial \theta}\frac{\partial \theta}{\partial z}$$

but

$$r = \sqrt{y^2 + z^2} \quad ; \quad \frac{\partial r}{\partial z} = \sin\theta$$

$$\theta = \tan^{-1}\frac{z}{y} \quad ; \quad \frac{\partial \theta}{\partial z} = \frac{\cos\theta}{r}$$

so

$$u_A = -\frac{\sin\theta}{r_o}\frac{\partial A_y}{\partial \rho} - \frac{\cos\theta}{r_o \rho}\frac{\partial A_y}{\partial \theta} \tag{9}$$

which we write as the total u perturbation due to the vector potential $\underline{A}$, since the trailing vortex does not contribute to this axial velocity component.

Similarly

$$v_{A_{bd}} = \underline{j} \cdot \underline{v_A} = 0$$

and

$$w_{A_{bd}} = \underline{k} \cdot \underline{v_A} = \frac{\partial A_y}{\partial x}$$

so

$$u_{r_{A_{bd}}} = w \sin\theta = \frac{\sin\theta}{r_o} \frac{\partial A_y}{\partial \xi} \qquad (10)$$

The radial perturbation velocity component u_{r_A} will also have a contribution from the trailing vortex, for which $A_y = A_z = 0$ For this case

$$u_{A_{tr}} = \underline{i} \cdot \underline{v_A} = 0$$

$$v_{A_{tr}} = \underline{j} \cdot \underline{v_A} = \frac{\partial A_x}{\partial z} = \frac{\partial A_x}{\partial r}\frac{\partial r}{\partial z} + \frac{\partial A_x}{\partial \theta}\frac{\partial \theta}{\partial z}$$

$$w_{A_{tr}} = \underline{k} \cdot \underline{v_A} = -\frac{\partial A_x}{\partial y} = -\frac{\partial A_x}{\partial r}\frac{\partial r}{\partial y} - \frac{\partial A_x}{\partial \theta}\frac{\partial \theta}{\partial y}$$

$$\frac{\partial r}{\partial z} = \sin\theta$$

$$\frac{\partial r}{\partial y} = \cos\theta$$

$$\frac{\partial \theta}{\partial z} = \frac{\cos\theta}{r}$$

$$\frac{\partial \theta}{\partial y} = -\frac{\sin\theta}{r}$$

$$v_{A_{tr}} = \sin\theta \frac{\partial A_x}{\partial r} + \frac{\cos\theta}{r} \frac{\partial A_x}{\partial \theta}$$

$$w_{A_{tr}} = -\cos\theta \frac{\partial A_x}{\partial r} + \frac{\sin\theta}{r} \frac{\partial A_x}{\partial \theta}$$

But

$$u_{r_{A_{tr}}} = v \cos\theta + w \sin\theta$$

Hence

$$u_{r_{A_{tr}}} = \frac{1}{r_o \rho} \frac{\partial A_x}{\partial \theta} \tag{11}$$

Now combining equations (10) and (11) we have the total radial perturbation velocity due to the vector potential $\underline{A}$:

$$u_{r_A} = \frac{\sin\theta}{r_o} \frac{\partial A_y}{\partial \xi} + \frac{1}{r_o \rho} \frac{\partial A_x}{\partial \theta} \tag{12}$$

These expressions (9) and (12) give the axial and radial velocity perturbations due to the horseshoe vortex whose vector potential is $\underline{A}$, in terms of the A_y and A_x components of the potential, corresponding to the bound and trailing elements of the horseshoe vortex.

We now proceed to determine these required components of the vector potential.

a. Bound Vortex Elements

We consider an elementary horseshoe vortex of strength

Γ lying in the plane $z = o$, of small but finite span extending between two parametric non-dimensionalized points c and d . The odd part is then of strength $\Gamma/2$. However, as can be seen from Figure 4, the bound vortex is of full strength Γ .

Now the flow due to a horseshoe vortex of strength Γ may be represented by the vector potential:

$$\underline{A} = \frac{\Gamma}{4\pi} \int \frac{d\,\underline{\ell}}{R'} \tag{13}$$

For a differential element of the bound vortex, $d\underline{\ell} = \underline{j}\, d\beta$, and $R' = \sqrt{\xi^2 + (\eta-\beta)^2 + \zeta^2}$, $A_x = A_z = 0$, and

$$dA_y = \frac{\Gamma d\beta}{4\pi} \quad \frac{1}{\sqrt{\xi^2 + (\eta-\beta)^2 + \zeta^2}}$$

Now we may represent the reciprocal distance by (Ref. 12, p. 75)

$$\frac{1}{R'} = \frac{1}{\sqrt{\xi^2 + (\eta-\beta)^2 + \zeta^2}} = \frac{2}{\pi} \int_o^\infty K_o\left[\lambda\sqrt{(\eta-\beta)^2 + \zeta^2}\right] \cos\xi\lambda d\lambda$$

Furthermore, from Figure 6

$$R = \sqrt{(\eta-\beta)^2 + \zeta^2} = \sqrt{\beta^2 + \rho^2 - 2\beta\rho\cos\theta}$$

Now applying Gegenbauer's addition theorem for $K_o(\lambda R)$ (Ref. 12, p. 74, Ref. 13, p. 44) for the case inside the jet, where $|\beta| < |\rho|$:

$$K_o(\lambda R) = I_o(\lambda\beta) K_o(\lambda\rho) + 2 \sum_{p=1}^{\infty} \cos p\theta\, I_p(\lambda\beta)\, K_p(\lambda\rho) \tag{14}$$

For $|\rho| < |\beta|$, interchange ρ and β . Thus $|\beta/\rho| < 1$

$$\frac{1}{R'} = \frac{2}{\pi}\int_0^\infty I_o(\lambda\beta)K_o(\lambda\rho)\cos\xi\lambda d\lambda + \sum_{p=1}^{\infty}\cos p\theta \cdot \frac{4}{\pi}\int_0^\infty I_p(\lambda\beta)K_p(\lambda\rho)\cos\xi\lambda d\lambda$$

For a pair of horseshoe vortices symmetrically spaced with respect to the jet axis, each of span from c to d , the terms for odd p cancel and those for even p combine, so

$$A_y = \frac{\Gamma}{\pi^2}\left[\int_0^\infty\left\{\int_c^d I_o(\lambda\beta)\,d\beta\right\}K_o(\lambda\rho)\cos\xi\lambda d\lambda\right.$$

$$\left. + 2\sum_{p=1}^{\infty}\cos 2p\theta\int_0^\infty\left\{\int_c^d I_{2p}(\lambda\beta)d\beta\right\}K_{2p}(\lambda\rho)\cos\xi\lambda d\lambda\right] \qquad (15)$$

b. Trailing Vortex Elements

Having found A_y , we may determine A_x by noting that the divergence of the vector potential $\underline{A}$ is zero, i.e.

$$\nabla \cdot \underline{A} = 0 \qquad (16)$$

$$\frac{\partial A_x}{\partial x} + \frac{\partial A_y}{\partial y} + \frac{\partial A_z}{\partial z} = 0$$

Since we are considering a vortex in the plane $z=o$, $A_z = o$. Hence we have:

$$\frac{\partial A_x}{\partial x} + \frac{\partial A_y}{\partial y} = 0 \qquad (17)$$

Now

$$\frac{\partial A_y}{\partial y} = \frac{\partial A_y}{\partial r}\,\frac{\partial r}{\partial y} + \frac{\partial A_y}{\partial \theta}\,\frac{\partial \theta}{\partial y}$$

$$\frac{\partial A_y}{\partial y} = \cos\theta\,\frac{\partial A_y}{\partial r} - \frac{\sin\theta}{r}\,\frac{\partial A_y}{\partial \theta}$$

$$\frac{\partial A_y}{\partial y} = \frac{\Gamma'}{\pi^2 r_o}\left[\cos\theta \int_o^\infty \left\{\int_c^d I_o(\lambda\beta)d\beta\right\} \lambda K_o'(\lambda\rho)\cos\xi\lambda d\lambda \right.$$

$$+ 2\sum_{p=1}^{\infty}\cos\theta\cos 2p\theta \int_o^\infty \left\{\int_c^d I_{2p}(\lambda\beta)\,d\beta\right\} \lambda K_{2p}'(\lambda\rho)\cos\xi\lambda d\lambda$$

$$\left. + \frac{2}{\rho}\sum_{p=1}^{\infty}(2p)\sin\theta\sin 2p\theta \int_o^\infty \left\{\int_c^d I_{2p}(\lambda\beta)\,d\beta\right\} K_{2p}(\lambda\rho)\cos\xi\lambda d\lambda\right]$$

But

$$\frac{\partial A_x}{\partial x} = -\frac{\partial A_y}{\partial y}$$

Hence

$$A_x = \int -\frac{\partial A_y}{\partial y}\,dx + f(r,\theta)$$

$$A_x = -\frac{\Gamma'}{\pi^2}\left[\cos\theta \int_o^\infty \left\{\int_c^d I_o(\lambda\beta)d\beta\right\} K_o'(\lambda\rho)\sin\lambda\xi d\lambda\right.$$

$$+ 2\sum_{p=1}^{\infty}\cos\theta\cos 2p\theta \int_o^\infty \left\{\int_c^d I_{2p}(\lambda\beta)d\beta\right\} K_{2p}'(\lambda\rho)\sin\lambda\xi d\lambda$$

$$\left. + \frac{2}{\rho}\sum_{p=1}^{\infty}(2p)\sin\theta\sin 2p\theta \int_o^\infty \left\{\int_c^d I_{2p}(\lambda\beta)d\beta\right\} \frac{1}{\lambda}K_{2p}(\lambda\rho)\sin\lambda\xi d\lambda\right]$$

$$+ f(\rho,\theta)$$

Now using:

$$2 \cos\theta \cos 2p\theta = \cos (2p+1)\theta + \cos (2p-1)\theta$$

$$2 \sin\theta \sin 2p\theta = \cos (2p-1)\theta - \cos (2p+1)\theta$$

$$A_x = -\frac{\Gamma}{\pi^2}\left[\cos\theta \int_0^\infty \left\{\int_c^d I_o(\lambda\beta)d\beta\right\} K_o'(\lambda\rho) \sin\xi\lambda d\lambda\right.$$

$$+\sum_{p=1}^{\infty}\left\{\cos(2p+1)\theta + \cos(2p-1)\theta\right\}\int_0^\infty\left\{\int_c^d I_{2p}(\lambda\beta)d\beta\right\}K_{2p}'(\lambda\rho)\sin\xi\lambda d\lambda$$

$$\left.+\sum_{p=1}^{\infty}\left\{\cos(2p-1)\theta-\cos(2p+1)\theta\right\}\int_0^\infty\left\{\int_c^d I_{2p}(\lambda\beta)d\beta\right\}\frac{2p}{\lambda\rho}K_{2p}(\lambda\rho)\sin\xi\lambda d\lambda\right] + f(\rho,\theta)$$

Combining terms, with

$$K_o' = -K_1$$

$$K_{2p}'(\lambda\rho) + \frac{2p}{\lambda\rho}K_{2p}(\lambda\rho) = -K_{2p-1}(\lambda\rho)$$

$$K_{2p}'(\lambda\rho) - \frac{2p}{\lambda\rho}K_{2p}(\lambda\rho) = -K_{2p+1}(\lambda\rho)$$

$$A_x = -\frac{\Gamma}{\pi^2}\left[-\cos\theta\int_0^\infty\left\{\int_c^d I_o(\lambda\beta)d\beta\right\}K_1(\lambda\rho)\sin\xi\lambda d\lambda\right.$$

$$-\sum_{p=1}^{\infty}\cos(2p-1)\theta\int_0^\infty\left\{\int_c^d I_{2p}(\lambda\beta)d\beta\right\}K_{2p-1}(\lambda\rho)\sin\xi\lambda d\lambda$$

$$\left.-\sum_{p=1}^{\infty}\cos(2p+1)\theta\int_0^\infty\left\{\int_c^d I_{2p}(\lambda\beta)d\beta\right\}K_{2p+1}(\lambda\rho)\sin\xi\lambda d\lambda\right] + f(\rho,\theta)$$

$$A_x = + \frac{\Gamma}{\pi^2} \left[\cos\theta \int_0^\infty \left\{ \int_c^d I_o(\lambda\beta)d\beta \right\} K_1(\lambda\rho) \sin \xi\lambda d\lambda \right.$$

$$+ \cos\theta \int_0^\infty \left\{ \int_c^d I_2(\lambda\beta)d\beta \right\} K_1(\lambda\rho) \sin \xi\lambda d\lambda$$

$$+ \sum_{p=2}^{\infty} \cos(2p-1)\theta \int_0^\infty \left\{ \int_c^d I_{2p}(\lambda\beta)d\beta \right\} K_{2p-1}(\lambda\rho) \sin \xi\lambda d\lambda$$

$$\left. + \sum_{p=1}^{\infty} \cos(2p+1)\theta \int_0^\infty \left\{ \int_c^d I_{2p}(\lambda\beta)d\beta \right\} K_{2p+1}(\lambda\rho) \sin \xi\lambda d\lambda \right] + f(\rho, \theta)$$

$$A_x = + \frac{\Gamma}{\pi^2} \left[\cos\theta \int_0^\infty \left\{ \int_c^d \left[I_o(\lambda\beta) + I_2(\lambda\beta) \right] d\beta \right\} K_1(\lambda\rho) \sin \xi\lambda d\lambda \right.$$

$$+ \sum_{p=1}^{\infty} \cos(2p+1)\theta \int_0^\infty \left\{ \int_c^d I_{2p+2}(\lambda\beta)d\beta \right\} K_{2p+1}(\lambda\rho) \sin \xi\lambda d\lambda$$

$$\left. + \sum_{p=1}^{\infty} \cos(2p+1)\theta \int_0^\infty \left\{ \int_c^d I_{2p}(\lambda\beta)d\beta \right\} K_{2p+1}(\lambda\rho) \sin \xi\lambda d\lambda \right] + f(\rho, \theta)$$

$$A_x = \frac{\Gamma}{\pi^2} \left[\cos\theta \int_0^\infty \left\{ \int_c^d \left[I_o(\lambda\beta) + I_2(\lambda\beta) \right] d\beta \right\} K_1(\lambda\rho) \sin \xi\lambda d\lambda \right.$$

$$\left. + \sum_{p=1}^{\infty} \cos(2p+1)\theta \int_0^\infty \left\{ \int_c^d \left[I_{2p}(\lambda\beta) + I_{2p+2}(\lambda\beta) \right] d\beta \right\} K_{2p+1}(\lambda\rho) \sin \xi\lambda d\lambda \right] + f(\rho, \theta)$$

$$A_x = \frac{\Gamma}{\pi^2} \sum_{p=o}^{\infty} \cos(2p+1)\theta \int_o^{\infty} \left\{ \int_c^d \left[I_{2p}(\lambda\beta) + I_{2p+2}(\lambda\beta) \right] d\beta \right\} K_{2p+1}(\lambda\rho) \sin \xi\lambda d\lambda \tag{18}$$

In this expression for A_x we have put $f(\rho, \theta) = 0$, since $f(\rho, \theta)$ is even in ξ, whereas A_x is odd in ξ, as seen from Equation (13) and Figure 4.

(1) Asymptotic Correlation with Even System

We may verify this expression for A_x by showing that the radial velocity obtained from it at $\xi = \pm \infty$ approaches the correct two-dimensional value. We will consider the particular case of $c = o$ to simplify the calculation. We have

$$2 I'_{2p+1} = I_{2p} + I_{2p+2}$$

Hence

$$\int_{c=o}^{d} \left[I_{2p}(\lambda\beta) + I_{2p+2}(\lambda\beta) \right] d\beta = \frac{1}{\lambda} \int_o^{d\lambda} 2 I'_{2p+1}(\lambda\beta) d(\lambda\beta)$$

$$= \frac{2}{\lambda} I_{2p+1}(\lambda\beta) \Big|_o^{d\lambda} = \frac{2}{\lambda} I_{2p+1}(\lambda d)$$

So:

$$A_x = \frac{2\Gamma}{\pi^2} \sum_{p=o}^{\infty} \cos(2p+1)\theta \int_o^{\infty} I_{2p+1}(\lambda d) K_{2p+1}(\lambda\rho) \frac{\sin \xi\lambda}{\lambda} d\lambda$$

The radial velocity is obtained from Eq. (11):

$$u_{r_{A_{tr}}} = \frac{1}{r_o \rho} \frac{\partial A_x}{\partial \theta} \tag{11}$$

$$u_{r_{A_{tr}}} = -\frac{2\Gamma}{r_o \rho \pi^2} \sum_{p=o}^{\infty} (2p+1)\sin(2p+1)\theta \int_o^{\infty} I_{2p+1}(\lambda d) K_{2p+1}(\lambda\rho) \frac{\sin\xi\lambda}{\lambda} d\lambda$$

Now consider the limit as $\xi \rightarrow \pm \infty$ of the integral

$$J = \int_0^\infty I_{2p+1}(\lambda d)\, K_{2p+1}(\lambda \rho)\, \frac{\sin \xi\lambda}{\lambda}\, d\lambda$$

Let

$$\xi\lambda = q \qquad d\lambda = \frac{dq}{\xi}$$

$$\lambda = \frac{q}{\xi} \qquad \frac{d\lambda}{\lambda} = \frac{dq}{q}$$

$$\lim_{\xi \rightarrow \pm \infty} \int_0^\infty I_{2p+1}\left(\frac{qd}{\xi}\right) K_{2p+1}\left(\frac{q\rho}{\xi}\right) \frac{\sin q}{q}\, dq$$

$$= \int_0^\infty \frac{\left(\frac{1}{2}\frac{qd}{\xi}\right)^{2p+1}}{(2p+1)!} \cdot \frac{1}{2} \frac{(2p+1-1)!}{1} \left(\frac{q\rho}{2\xi}\right)^{-2p-1} \frac{\sin q}{q}\, dq$$

$$= \frac{1}{2} \frac{1}{2p+1} \left(\frac{d}{\rho}\right)^{2p+1} \int_0^\infty \frac{\sin q}{q}\, dq$$

Hence

$$J = \frac{1}{2} \frac{1}{2p+1} \left(\frac{d}{\rho}\right)^{2p+1} \left(\pm \frac{\pi}{2}\right)$$

\+ when $\xi \rightarrow +\infty$

\- when $\xi \rightarrow -\infty$

And

$$u_{r_{A_{tr}}} = \mp \frac{\Gamma}{2r_o\rho\pi} \sum_{p=o}^{\infty} \left(\frac{d}{\rho}\right)^{2p+1} \sin (2p+1)\,\theta$$

$$= \mp \frac{\Gamma}{2\pi r_o \rho} \sum_{p=o}^{\infty} \frac{d^{2p+1}}{\rho^{2p+1}} \left[\frac{e^{i(2p+1)\theta} - e^{-i(2p+1)\theta}}{2i} \right]$$

Now summing this geometric series in the form x^{2p}:

$$u_{r_{A_{tr}}} = \mp \frac{\Gamma}{4\pi r_o \rho i} \left[\frac{\frac{d}{\rho} e^{i\theta}}{1 - \frac{d^2}{\rho^2} e^{2i\theta}} - \frac{\frac{d}{\rho} e^{-i\theta}}{1 - \frac{d^2}{\rho^2} e^{-2i\theta}} \right]$$

$$u_{r_{A_{tr}}} = \mp \frac{\Gamma d \sin\theta}{2\pi r_o} \left[\frac{\rho^2 + d^2}{\rho^4 + d^4 - 2\rho^2 d^2 \cos 2\theta} \right] \begin{matrix} - \text{ when } \xi \longrightarrow + \infty \\ + \text{ when } \xi \longrightarrow - \infty \end{matrix} \qquad (19)$$

To check this result, we now obtain the two-dimensional radial velocity directly, using $\Gamma/2$ as the strength of the even half of the flow. For the particular case treated, where c = o, the pair of horseshoe vortices symmetrically spaced about the axis reduce to a single horseshoe vortex symmetrically spaced about the axis at semi-span d:

From Figure 7 we note

$$\delta = \eta + i\zeta = \rho e^{i\theta}$$

The complex potential is then

$$F(\delta) = \frac{i\,\Gamma/2}{2\pi} \left[\log (\delta - d) - \log (\delta + d) \right]$$

$$\mp\Phi + i\Psi = \frac{i\Gamma}{4\pi} \left[\log \left| \frac{\delta - d}{\delta + d} \right| + i \arg \left(\frac{\delta - d}{\delta + d} \right) \right]$$

$$\Psi = \frac{\Gamma}{4\pi} \log \left| \frac{\delta - d}{\delta + d} \right| = \frac{\Gamma}{4\pi} \log \frac{\sqrt{(\eta - d)^2 + \zeta^2}}{\sqrt{(\eta + d)^2 + \zeta^2}}$$

$$= \frac{\Gamma}{8\pi} \log \frac{(\rho \cos\theta - d)^2 + \rho^2 \sin^2\theta}{(\rho \cos\theta + d)^2 + \rho^2 \sin^2\theta}$$

$$\Psi = \frac{\Gamma}{8\pi}\left[\log\left(\rho^2 + d^2 - 2\rho d\cos\theta\right) - \log\left(\rho^2 + d^2 + 2\rho d\cos\theta\right)\right]$$

$$u_{r_{A_{tr}}} = \frac{1}{r_o\,\rho}\,\frac{\partial\Psi}{\partial\theta} = \frac{\Gamma}{8\pi r_o\,\rho}\left[\frac{+2\rho d\sin\theta}{\rho^2 + d^2 - 2\rho d\cos\theta} - \frac{-2\rho d\sin\theta}{\rho^2 + d^2 + 2\rho d\cos\theta}\right]$$

$$u_{r_{A_{tr}}} = \frac{\Gamma d\sin\theta}{4\pi r_o}\left[\frac{2(\rho^2 + d^2)}{(\rho^2 + d^2)^2 - 4\rho^2 d^2\cos^2\theta}\right]$$

Now consider the denominator, using $2\cos^2\theta = 1 + \cos 2\theta$

$$(\rho^2 + d^2)^2 - 2\rho^2 d^2\,(1 + \cos 2\theta)$$

$$= \rho^4 + d^4 - 2\rho^2 d^2\cos 2\theta$$

Hence:

$$u_{r_{A_{tr}}} = + \frac{\Gamma d\sin\theta}{2\pi r_o}\left[\frac{\rho^2 + d^2}{\rho^4 + d^4 - 2\rho^2 d^2\cos 2\theta}\right] \left(\begin{matrix}\text{Two}\\ \text{dimensional}\end{matrix}\right) \qquad (20)$$

This expression (20) for the even part is identical with (19) which was obtained in the limit as $\xi \longrightarrow \pm\infty$ from the A_x potential of the odd part. The signs are identical when $\xi = -\infty$, which is where the odd part should approach and add to the even part. When $\xi = +\infty$, the signs are opposite, so the odd and even parts cancel, giving the correct representation of no vortex upstream.

This verifies that the expression for A_x given by Eq. (18) is the odd part of strength $\Gamma/2$.

c. Application of Boundary Conditions

We now have expressions for A_y and A_x, which are known functions. We have series representations for the potentials ϕ of the flow due to the boundary, unknown to the extent of a coefficient in each of the two expressions. By employing the two boundary conditions (1) and (2), we may determine these two coefficients and hence determine the potentials ϕ for the flow due to the boundary in the two regions.

(1) Pressure Boundary Condition

The first boundary condition which applies on the surface $\rho = 1$ is:

$$V_j u_j = V_o u_o \tag{1}$$

which on employing Eq. (9) becomes:

$$-V_j\left[-\frac{\sin\theta}{r_o}\frac{\partial A_y}{\partial\rho}-\frac{\cos\theta}{r_o\rho}\frac{\partial A_y}{\partial\theta}+\frac{\partial\phi}{r_o\partial\xi}\right]_j=-V_o\left[-\frac{\sin\theta}{r_o}\frac{\partial A_y}{\partial\rho}-\frac{\cos\theta}{r_o\rho}\frac{\partial A_y}{\partial\theta}+\frac{\partial\phi}{r_o\partial\xi}\right]_o$$

Now since the form of the vector potential depends only on the location of the real horseshoe vortex and not on the effect region, we may write

$$\left\{-V_j+V_o\right\}\left[-\frac{\sin\theta}{r_o}\frac{\partial A_y}{\partial\rho}-\frac{\cos\theta}{r_o\rho}\frac{\partial A_y}{\partial\theta}\right]_j - V_j\left[\frac{\partial\phi}{r_o\partial\xi}\right]_j=-V_o\left[\frac{\partial\phi}{r_o\partial\xi}\right]_o$$

On substituting the potentials from Eqs. (15), (6), and (7), and putting $\rho = 1$, we have

$$\left\{-V_j + V_o\right\}\left[-\frac{\sin\theta}{r_o}\frac{\Gamma}{\pi^2}\int_o^\infty\left\{\int_c^d I_o(\lambda\beta)d\beta\right\}\lambda K_o'(\lambda)\cos\xi\lambda d\lambda\right.$$

$$-\frac{\sin\theta}{r_o}\frac{\Gamma}{\pi^2}\cdot 2\sum_{p=1}^{\infty}\cos 2p\theta\int_o^\infty\left\{\int_c^d I_{2p}(\lambda\beta)d\beta\right\}\lambda K_{2p}'(\lambda)\cos\xi\lambda d\lambda$$

$$\left.+\frac{\cos\theta}{r_o}\frac{\Gamma}{\pi^2}\cdot 2\sum_{p=1}^{\infty}(2p)\sin 2p\theta\int_o^\infty\left\{\int_c^d I_{2p}(\lambda\beta)d\beta\right\}K_{2p}(\lambda)\cos\xi\lambda d\lambda\right]$$

$$-V_j\left[\frac{1}{r_o}\frac{2\Gamma}{\pi^2}\sum_{p=o}^{\infty}\sin(2p+1)\theta\int_o^\infty A_{2p+1}(\lambda)\,I_{2p+1}(\lambda)\,\lambda\cos\xi\lambda d\lambda\right]$$

$$=-V_o\left[\frac{1}{r_o}\frac{2\Gamma}{\pi^2}\sum_{p=o}^{\infty}\sin(2p+1)\theta\int_o^\infty B_{2p+1}(\lambda)\,K_{2p+1}(\lambda)\,\lambda\cos\xi\lambda d\lambda\right]$$

Now we divide through by $-\frac{\Gamma}{\pi^2 r_o}$, take the Fourier cosine transform with respect to ξ, and divide through by λ. In this expression and the following analysis, the omission of the argument of a Bessel function or the coefficients A and B means the argument is λ:

$$\left\{ V_j - V_o \right\} \left[- \sin\theta \left\{ \int_c^d I_o(\lambda\beta)d\beta \right\} K_o' \right.$$

$$- 2 \sum_{p=1}^{\infty} \sin\theta \cos 2p\theta \left\{ \int_c^d I_{2p}(\lambda\beta)d\beta \right\} K_{2p}'$$

$$\left. + 2 \sum_{p=1}^{\infty} \cos\theta \sin 2p\theta \left\{ \int_c^d I_{2p}(\lambda\beta)d\beta \right\} \frac{2p}{\lambda} K_{2p} \right]$$

$$+ V_j \left[2 \sum_{p=o}^{\infty} \sin(2p+1)\theta \; A_{2p+1} I_{2p+1} \right]$$

$$= V_o \left[2 \sum_{p=o}^{\infty} \sin(2p+1)\theta \; B_{2p+1} K_{2p+1} \right]$$

We may now simplify the terms in the first square bracket as follows,

$$2 \sin\theta \cos 2p\theta = \sin(2p+1)\theta - \sin(2p-1)\theta$$

using

$$2 \cos\theta \sin 2p\theta = \sin(2p+1)\theta + \sin(2p-1)\theta$$

and obtaining:

$$- \sin\theta \left\{ \int_c^d I_o(\lambda\beta)d\beta \right\} K_o'$$

$$+ \sum_{p=1}^{\infty} \left\{ - \sin(2p+1)\theta + \sin(2p-1)\theta \right\} \left\{ \int_c^d I_{2p}(\lambda\beta)d\beta \right\} K_{2p}'$$

$$+ \sum_{p=1}^{\infty} \left\{ \sin(2p+1)\theta + \sin(2p-1)\theta \right\} \left\{ \int_c^d I_{2p}(\lambda\beta)d\beta \right\} \frac{2p}{\lambda} K_{2p}$$

Next using:

$$K_{2p}'(\lambda) + \frac{2p}{\lambda} K_{2p}(\lambda) = - K_{2p-1}(\lambda)$$

$$-K_{2p}'(\lambda) + \frac{2p}{\lambda} K_{2p}(\lambda) = + K_{2p+1}(\lambda)$$

we obtain:

$$+ \sin\theta \left\{ \int_c^d I_o(\lambda\beta)d\beta \right\} K_1$$

$$- \sum_{p=1}^{\infty} \sin(2p-1)\theta \left\{ \int_c^d I_{2p}(\lambda\beta)d\beta \right\} K_{2p-1}$$

$$+ \sum_{p=1}^{\infty} \sin(2p+1)\theta \left\{ \int_c^d I_{2p}(\lambda\beta)d\beta \right\} K_{2p+1}$$

Then:

$$\sin\theta \left\{ \int_c^d I_o(\lambda\beta)d\beta \right\} K_1$$

$$-\sin\theta \left\{ \int_c^d I_2(\lambda\beta)d\beta \right\} K_1$$

$$- \sum_{p=2}^{\infty} \sin(2p-1)\theta \left\{ \int_c^d I_{2p}(\lambda\beta)d\beta \right\} K_{2p-1}$$

$$+ \sum_{p=1}^{\infty} \sin(2p+1)\theta \left\{ \int_c^d I_{2p}(\lambda\beta)d\beta \right\} K_{2p+1}$$

Then:

$$\sin\theta \int_c^d \left\{ I_o(\lambda\beta) - I_2(\lambda\beta) \right\} d\beta \, K_1$$

$$- \sum_{p=1}^{\infty} \sin(2p+1)\theta \left\{ \int_c^d I_{2p+2}(\lambda\beta)d\beta \right\} K_{2p+1}$$

$$+ \sum_{p=1}^{\infty} \sin(2p+1)\theta \left\{ \int_c^d I_{2p}(\lambda\beta)d\beta \right\} K_{2p+1}$$

Then:

$$\sin\theta \int_c^d \left\{ I_o(\lambda\beta) - I_2(\lambda\beta) \right\} d\beta \, K_1$$

$$+ \sum_{p=1}^{\infty} \sin(2p+1)\theta \left\{ \int_c^d \left[I_{2p}(\lambda\beta) - I_{2p+2}(\lambda\beta) \right] d\beta \right\} K_{2p+1}$$

Then

$$\sum_{p=o}^{\infty} \sin (2p+1)\,\theta \left\{ \int_{c}^{d} \left[I_{2p}(\lambda\beta) - I_{2p+2}(\lambda\beta) \right] d\beta \right\} K_{2p+1}$$

Finally:

$$\frac{2}{\lambda} \sum_{p=o}^{\infty} (2p+1) \sin (2p+1)\,\theta \; K_{2p+1} \int_{c\lambda}^{d\lambda} \frac{I_{2p+1}(\lambda\beta)}{\lambda\beta} d(\lambda\beta)$$

The complete equation then becomes:

$$\left\{ V_j - V_o \right\} \frac{2}{\lambda} \sum_{p=o}^{\infty} (2p+1) \sin (2p+1)\,\theta \; K_{2p+1} \int_{c\lambda}^{d\lambda} \frac{I_{2p+1}(\lambda\beta)}{\lambda\beta} d(\lambda\beta)$$

$$+ 2 V_j \sum_{p=o}^{\infty} \sin (2p+1)\,\theta \; A_{2p+1} I_{2p+1} = 2V_o \sum_{p=o}^{\infty} \sin (2p+1)\theta \; B_{2p+1} K_{2p+1}$$

This equation must hold for all values of θ, hence we may equate coefficients of $\sin (2p+1)\theta$, where p runs from 0 to ∞. Also, since now all Bessel functions and the functions A and B are of order 2p+1, we drop the subscript temporarily:

$$\left\{ V_j - V_o \right\} \frac{2}{\lambda} (2p+1) K \int_{c\lambda}^{d\lambda} \frac{I(\lambda\beta)}{\lambda\beta} d(\lambda\beta) + 2V_j A I = 2V_o BK \qquad (21)$$

(2) Kinematic Boundary Condition

The second boundary condition which applies on the surface $\rho = 1$ is:

$$V_o \, u_{r_j} = V_j \, u_{r_o} \tag{2}$$

which on employing Eq. (12) becomes:

$$-V_o \left[\frac{\sin\theta}{r_o} \frac{\partial A_y}{\partial \xi} + \frac{1}{r_o \rho} \frac{\partial A_x}{\partial \theta} + \frac{\partial \phi}{r_o \partial \rho} \right]_j = -V_j \left[\frac{\sin\theta}{r_o} \frac{\partial A_y}{\partial \xi} + \frac{1}{r_o \rho} \frac{\partial A_x}{\partial \theta} + \frac{\partial \phi}{r_o \partial \rho} \right]_o$$

which as before may be written:

$$\left\{ -V_o + V_j \right\} \left[\frac{\sin\theta}{r_o} \frac{\partial A_y}{\partial \xi} + \frac{1}{r_o \rho} \frac{\partial A_x}{\partial \theta} \right]_j - V_o \left[\frac{\partial \phi}{r_o \partial \rho} \right]_j = - V_j \left[\frac{\partial \phi}{r_o \partial \rho} \right]_o$$

On substituting the potentials from Eqs. (15), (18), (6) and (7), and putting $\rho = 1$, we have:

$$\left\{ -V_o + V_j \right\} \left[- \frac{\sin\theta}{r_o} \frac{\Gamma}{\pi^2} \int_o^\infty \left\{ \int_c^d I_o(\lambda\beta) d\beta \right\} \lambda K_o(\lambda) \sin \xi\lambda d\lambda \right.$$

$$- \frac{\sin\theta}{r_o} \frac{\Gamma}{\pi^2} 2 \sum_{p=1}^{\infty} \cos 2p\theta \int_o^\infty \left\{ \int_c^d I_{2p}(\lambda\beta) d\beta \right\} \lambda K_{2p}(\lambda) \sin \xi\lambda d\lambda$$

$$- \frac{1}{r_o} \frac{\Gamma}{\pi^2} \sum_{p=o}^{\infty} (2p+1) \sin(2p+1)\theta \int_o^\infty \left\{ \int_c^d \left[I_{2p}(\lambda\beta) + I_{2p+2}(\lambda\beta) \right] d\beta \right\} K_{2p+1}(\lambda)$$

$$\left. \sin \xi\lambda d\lambda \right]$$

$$-V_o \left[\frac{1}{r_o} \frac{2\Gamma}{\pi^2} \sum_{p=o}^{\infty} \sin (2p+1)\theta \int_o^\infty \lambda \, A_{2p+1}(\lambda) \, I'_{2p+1}(\lambda) \sin \xi\lambda d\lambda \right]$$

$$= -V_j \left[\frac{1}{r_o} \frac{2\Gamma}{\pi^2} \sum_{p=o}^{\infty} \sin (2p+1)\theta \int_o^\infty \lambda \, B_{2p+1}(\lambda) K'_{2p+1}(\lambda) \sin \xi\lambda d\lambda \right]$$

As before we divide through by $-\frac{\Gamma}{\pi^2 r_o}$, take the Fourier sine transform with respect to ξ, and divide through by λ :

$$\left\{V_o - V_j\right\}\left[-\sin\theta\left\{\int_c^d I_o(\lambda\beta)d\beta\right\}K_o\right.$$

$$-2\sum_{p=1}^{\infty}\sin\theta\cos 2p\theta\left\{\int_c^d I_{2p}(\lambda\beta)d\beta\right\}K_{2p}$$

$$\left.-\sum_{p=o}^{\infty}\sin(2p+1)\theta\left\{\int_c^d\left[I_{2p}(\lambda\beta)+I_{2p+2}(\lambda\beta)\right]d\beta\right\}\frac{2p+1}{\lambda}K_{2p+1}\right]$$

$$+V_o\left[2\sum_{p=o}^{\infty}\sin(2p+1)\theta\,A_{2p+1}I'_{2p+1}\right]$$

$$=V_j\left[2\sum_{p=o}^{\infty}\sin(2p+1)\theta\,B_{2p+1}K'_{2p+1}\right]$$

Simplifying the terms in the first square bracket, using

$$2\sin\theta\cos 2p\theta=\sin(2p+1)\theta-\sin(2p-1)\theta$$

we obtain

$$-\sin\theta\left\{\int_c^d I_o(\lambda\beta)d\beta\right\}K_o$$

$$-\sum_{p=1}^{\infty}\left\{\sin(2p+1)\theta-\sin(2p-1)\theta\right\}\left\{\int_c^d I_{2p}(\lambda\beta)d\beta\right\}K_{2p}$$

$$-\sum_{p=o}^{\infty}\sin(2p+1)\theta\left\{\int_c^d\left[I_{2p}(\lambda\beta)+I_{2p+2}(\lambda\beta)\right]d\beta\right\}\frac{2p+1}{\lambda}K_{2p+1}$$

Then:

$$- \sin\theta\left\{\int_c^d I_o(\lambda\beta)d\beta\right\} K_o + \sin\theta\left\{\int_c^d I_2(\lambda\beta)d\beta\right\} K_2$$

$$+ \sum_{p=2}^{\infty} \sin(2p-1)\,\theta\left\{\int_c^d I_{2p}(\lambda\beta)d\beta\right\} K_{2p}$$

$$- \sum_{p=1}^{\infty} \sin(2p+1)\theta\left\{\int_c^d I_{2p}(\lambda\beta)d\beta\right\} K_{2p}$$

$$- \sum_{p=o}^{\infty} \sin(2p+1)\,\theta\left\{\int_c^d \left[I_{2p}(\lambda\beta) + I_{2p+2}(\lambda\beta)\right] d\beta\right\} \frac{2p+1}{\lambda} K_{2p+1}$$

Now using

$$-\frac{1}{\lambda} K_1 - K_o = + K_1'$$

$$-\frac{1}{\lambda} K_1 + K_2 = - K_1'$$

we obtain:

$$\sin\theta\left\{\int_c^d I_o(\lambda\beta)d\beta\right\} K_1' - \sin\theta\left\{\int_c^d I_2(\lambda\beta)d\beta\right\} K_1'$$

$$+ \sum_{p=1}^{\infty} \sin(2p+1)\,\theta\left\{\int_c^d I_{2p+2}(\lambda\beta)d\beta\right\} K_{2p+2}$$

$$- \sum_{p=1}^{\infty} \sin(2p+1)\,\theta\left\{\int_c^d I_{2p}(\lambda\beta)d\beta\right\} K_{2p}$$

$$- \sum_{p=1}^{\infty} \sin(2p+1)\,\theta\left\{\int_c^d \left[I_{2p}(\lambda\beta) + I_{2p+2}(\lambda\beta)\right] d\beta\right\} \frac{2p+1}{\lambda} K_{2p+1}$$

Also:

$$-\frac{2p+1}{\lambda} K_{2p+1} - K_{2p} = + K_{2p+1}'$$

$$-\frac{2p+1}{\lambda} K_{2p+1} + K_{2p+2} = - K_{2p+1}'$$

gives:

$$\sin\theta\left\{\int_c^d \left[I_o(\lambda\beta) - I_2(\lambda\beta)\right] d\beta\right\} K_1'$$

$$+ \sum_{p=1}^{\infty} \sin(2p+1)\theta\left\{\int_c^d I_{2p}(\lambda\beta)\, d\beta\right\} K'_{2p+1}$$

$$- \sum_{p=1}^{\infty} \sin(2p+1)\theta\left\{\int_c^d I_{2p+2}(\lambda\beta)\, d\beta\right\} K'_{2p+1}$$

Then:

$$\sum_{p=o}^{\infty} \sin(2p+1)\theta\left\{\int_c^d \left[I_{2p}(\lambda\beta) - I_{2p+2}(\lambda\beta)\right] d\beta\right\} K'_{2p+1}$$

Finally: $\frac{2}{\lambda} \sum_{p=o}^{\infty} (2p+1) \sin(2p+1)\theta\, K'_{2p+1} \int_{c\lambda}^{d\lambda} \frac{I_{2p+1}(\lambda\beta)}{\lambda\beta}\, d(\lambda\beta)$

The complete equation then becomes:

$$\left\{V_o - V_j\right\} \frac{2}{\lambda} \sum_{p=o}^{\infty} (2p+1) \sin(2p+1)\theta\, K'_{2p+1} \int_{c\lambda}^{d\lambda} \frac{I_{2p+1}(\lambda\beta)}{\lambda\beta}\, d(\lambda\beta)$$

$$+ 2V_o \sum_{p=o}^{\infty} \sin(2p+1)\theta\, A_{2p+1} I'_{2p+1} = 2V_j \sum_{p=o}^{\infty} \sin(2p+1)\theta B_{2p+1} K'_{2p+1}$$

Equating coefficients of $\sin(2p+1)\theta$, we have

$$\left\{V_o - V_j\right\} \frac{2}{\lambda} (2p+1) K' \int_{c\lambda}^{d\lambda} \frac{I(\lambda\beta)}{\lambda\beta} d(\lambda\beta) + 2V_o A I' = 2V_j B K' \qquad (22)$$

d. Results

We now have two equations for the two unknowns A and B :

$$\left\{V_j - V_o\right\} \frac{2}{\lambda} (2p+1) K \int_{c\lambda}^{d\lambda} \frac{I(\lambda\beta)}{\lambda\beta} d(\lambda\beta) + 2V_j A I = 2V_o B K \tag{21}$$

$$\left\{V_o - V_j\right\} \frac{2}{\lambda} (2p+1) K' \int_{c\lambda}^{d\lambda} \frac{I(\lambda\beta)}{\lambda\beta} d(\lambda\beta) + 2V_o A I' = 2V_j B K' \tag{22}$$

Solving for the coefficients A and B , using

$$W = \begin{vmatrix} I & K \\ I' & K' \end{vmatrix} = IK' - I'K = -\frac{1}{\lambda}$$

we obtain:

$$B_{2p+1}(\lambda) = \left[\frac{V_o V_j}{\lambda} \frac{1}{V_o^2 I'K - V_j^2 IK'} - 1\right] \frac{2p+1}{\lambda} \int_{c\lambda}^{d\lambda} \frac{I(\lambda\beta)}{\lambda\beta} d(\lambda\beta) \tag{23}$$

$$A_{2p+1}(\lambda) = \frac{2p+1}{\lambda} \frac{\left\{V_j^2 - V_o^2\right\} KK'}{V_o^2 I'K - V_j^2 IK'} \int_{c\lambda}^{d\lambda} \frac{I(\lambda\beta)}{\lambda\beta} d(\lambda\beta) \tag{24}$$

Substituting the values of A and B in the expressions for the potentials, Eqs. (6) and (7), for the case of a horseshoe vortex inside a jet, where all Bessel functions are of the 2p+1 order:

$$\phi_{jj} = \frac{2\Gamma}{\pi^2} \sum_{p=o}^{\infty} (2p+1)\sin(2p+1)\theta \int_o^{\infty} \frac{\left\{V_j^2 - V_o^2\right\} KK' I(\lambda\rho)}{V_o^2 I'K - V_j^2 IK'} \frac{\sin\xi\lambda d\lambda}{\lambda} \int_{c\lambda}^{d\lambda} \frac{I(\lambda\beta)}{\lambda\beta} d(\lambda\beta) \tag{6a}$$

$$\phi_{oj} = \frac{2\Gamma}{\pi^2} \sum_{p=o}^{\infty} (2p+1)\sin(2p+1)\theta \int_o^{\infty} \left[\frac{V_o V_j}{\lambda} \frac{1}{V_o^2 I'K - V_j^2 IK'} - 1\right] \frac{K(\lambda\rho)\sin\xi\lambda d\lambda}{\lambda} \int_{c\lambda}^{d\lambda} \frac{I(\lambda\beta)}{\lambda\beta} d(\lambda\beta) \tag{7a}$$

B. Horseshoe Vortex Outside Jet

The elementary horseshoe vortex outside the jet may be treated in a manner identical to the vortex inside.

1. Even System

As before, the even system, as illustrated in Figure 8, is two-dimensional. A similar image system may be used, consisting of image vortices located inside the jet at the inverse points, as illustrated in Figure 9.

For this case, when a real vortex is located outside the jet, it has been shown (Ref. 1, p. 389) that the contribution to the motion outside the jet due to the boundary, is that represented by the fictitious image system inside the boundary, modified in intensity by the factor $-\frac{V_j^2 - V_o^2}{V_j^2 + V_o^2}$. Thus when the outer velocity V_o is zero, the image strength is equal in magnitude and opposite in sign to the real vortex outside the jet. As V_o approaches V_j, the image strength vanishes with the boundary.

The contribution of the boundary to the motion inside the jet, due to a real vortex located outside the jet, in the presence of a boundary, is that of the real vortex itself, modified in intensity

by the factor $-\frac{(V_j - V_o)^2}{V_j^2 + V_o^2}$. When the outer velocity V_o is zero, this boundary contribution is undiminished, and completely cancels the real vortex outside. As V_o approaches V_j, the boundary vanishes, and the effect of the real vortex outside is undiminished.

a. Effect Inside Jet

The downwash induced at a point η inside the jet by the boundary due to a pair of real line vortices of strength $\Gamma/2$ extending to $\pm\infty$ through points c and d is:

$$w_{jo}(\eta) = \frac{\Gamma}{4\pi r_o}\left[\frac{1}{d-\eta} - \frac{1}{c-\eta}\right]$$

and that induced by the vortex pair at -c and -d is:

$$w_{jo}(\eta) = \frac{\Gamma}{4\pi r_o}\left[\frac{1}{d+\eta} - \frac{1}{c+\eta}\right]$$

Hence for a pair of finite horseshoe vortices, symmetrically spaced with respect to the axis of the jet, the downwash induced by the boundary, due to the even part, at a point η inside the jet, taking into account the image strength factor, is:

$$w_{jo}(\eta) = -\frac{(V_j - V_o)^2}{V_j^2 + V_o^2}\,\frac{\Gamma}{4\pi r_o}\left[\frac{1}{d-\eta} - \frac{1}{c-\eta} + \frac{1}{d+\eta} - \frac{1}{c+\eta}\right] \qquad (25)$$

b. Effect Outside Jet

For a pair of real line vortices extending to $\pm\infty$ through points c and d, the image line vortices will extend through the inverse points of c and d, namely $\frac{1}{c}$ and $\frac{1}{d}$ respectively.

The downwash induced at a point η outside the jet due to the image vortex pair located at the inverse points of c and d is:

$$w_{oo}(\eta) = \frac{\Gamma}{4\pi r_o}\left[-\frac{1}{\eta - \frac{1}{d}} + \frac{1}{\eta - \frac{1}{c}}\right]$$

and for the image pair located at the inverse points of -c and -d :

$$w_{oo}(\eta) = \frac{\Gamma}{4\pi r_o}\left[-\frac{1}{\eta + \frac{1}{c}} + \frac{1}{\eta + \frac{1}{d}}\right]$$

Hence for a pair of finite horseshoe vortices, symmetrically spaced with respect to the axis of the jet, the downwash due to the image of the even part, induced at a point η outside the jet, taking into account the image strength factor, is:

$$w_{oo}(\eta) = -\frac{V_j^2 - V_o^2}{V_j^2 + V_o^2}\,\frac{\Gamma}{4\pi r_o}\left[-\frac{1}{\eta - \frac{1}{d}} + \frac{1}{\eta - \frac{1}{c}} - \frac{1}{\eta + \frac{1}{c}} + \frac{1}{\eta + \frac{1}{d}}\right] \tag{26}$$

2. Odd System

As before, we represent the total perturbation velocity $\underline{v}$ for the odd system (2) of Figure 8 by the sum:

$$\underline{v} = \nabla \times \underline{A} + \nabla \phi \tag{5}$$

where for $\rho < 1$

$$\phi_j = \frac{2\Gamma}{\pi^2} \sum_{p=o}^{\infty} \sin (2p+1)\theta \int_o^{\infty} A_{2p+1}(\lambda)\, I_{2p+1}(\lambda\rho) \sin \xi\lambda d\lambda \tag{6}$$

and for $\rho > 1$

$$\phi_o = \frac{2\Gamma}{\pi^2} \sum_{p=o}^{\infty} \sin (2p+1)\theta \int_o^{\infty} B_{2p+1}(\lambda) K_{2p+1}(\lambda\rho) \sin \xi\lambda d\lambda \tag{7}$$

The expressions for the known perturbation velocities due to the vector potential $\underline{A}$ are unchanged, as given in Eqs. (9) and (12).

a. Bound Vortex Elements

We consider the bound vortex as before, interchanging ρ and β in Gegenbauer's addition theorem in Eq. (14). Hence for $|\beta| > |\rho|$:

$$K_o(\lambda R) = I_o(\lambda\rho)\, K_o(\lambda\beta) + 2 \sum_{p=1}^{\infty} \cos p\theta\, I_p(\lambda\rho) K_p(\lambda\beta) \tag{14a}$$

Thus for $|\beta/\rho| > 1$

$$\frac{1}{R} = \frac{2}{\pi} \int_0^{\infty} I_o(\lambda\rho) K_o(\lambda\beta) \cos\xi\lambda d\lambda + \sum_{p=1}^{\infty} \cos p\theta \cdot \frac{4}{\pi} \int_0^{\infty} I_p(\lambda\rho) K_p(\lambda\beta) \cos\xi\lambda d\lambda$$

For a pair of horseshoe vortices symmetrically spaced with respect to the jet axis, each of span from c to d, the terms for odd p cancel and those for even p combine, so

$$A_y = \frac{\Gamma}{\pi^2} \left[\int_0^{\infty} \left\{ \int_c^d K_o(\lambda\beta) d\beta \right\} I_o(\lambda\rho) \cos\xi\lambda d\lambda \right.$$

$$\left. + 2 \sum_{p=1}^{\infty} \cos 2p\theta \int_0^{\infty} \left\{ \int_c^d K_{2p}(\lambda\beta) d\beta \right\} I_{2p}(\lambda\rho) \cos\xi\lambda d\lambda \right] \tag{27}$$

b. Trailing Vortex Elements

As before, we obtain A_x from A_y, employing the divergence theorem (16) and (17).

Now:

$$\frac{\partial A_y}{\partial y} = \cos\theta \frac{\partial A_y}{\partial r} - \frac{\sin\theta}{r} \frac{\partial A_y}{\partial \theta}$$

$$\frac{\partial A_y}{\partial y} = \frac{\Gamma}{\pi^2 r_o} \left[\cos\theta \int_o^\infty \left\{ \int_c^d K_o(\lambda\beta)d\beta \right\} \lambda I_o'(\lambda\rho) \cos\xi\lambda d\lambda \right.$$

$$+ 2 \sum_{p=1}^{\infty} \cos\theta \cos 2p\theta \int_o^\infty \left\{ \int_c^d K_{2p}(\lambda\beta)d\beta \right\} \lambda I_{2p}'(\lambda\rho) \cos\xi\lambda d\lambda$$

$$\left. + \frac{2}{\rho} \sum_{p=1}^{\infty} (2p) \sin\theta \sin 2p\theta \int_o^\infty \left\{ \int_c^d K_{2p}(\lambda\beta)d\beta \right\} I_{2p}(\lambda\rho) \cos\xi\lambda d\lambda \right]$$

And:

$$A_x = \int - \frac{\partial A_y}{\partial y} dx + g(r,\theta)$$

$$A_x = -\frac{\Gamma}{\pi^2} \left[\cos\theta \int_o^\infty \left\{ \int_c^d K_o(\lambda\beta)d\beta \right\} I_o'(\lambda\rho) \sin\xi\lambda d\lambda \right.$$

$$+ \sum_{p=1}^{\infty} \left\{ \cos(2p+1)\theta + \cos(2p-1)\theta \right\} \int_o^\infty \left\{ \int_c^d K_{2p}(\lambda\beta)d\beta \right\} I_{2p}'(\lambda\rho) \sin\xi\lambda d\lambda$$

$$\left. + \sum_{p=1}^{\infty} \left\{ \cos(2p-1)\theta - \cos(2p+1)\theta \right\} \int_o^\infty \left\{ \int_c^d K_{2p}(\lambda\beta)d\beta \right\} \frac{2p}{\lambda\rho} I_{2p}(\lambda\rho) \sin\xi\lambda d\lambda \right]$$

$$+ g(\rho,\theta)$$

Combining terms, with

$$I_o' = I_1$$

$$I_{2p}'(\lambda\rho) + \frac{2p}{\lambda\rho} I_{2p}(\lambda\rho) = I_{2p-1}(\lambda\rho)$$

$$I_{2p}'(\lambda\rho) - \frac{2p}{\lambda\rho} I_{2p}(\lambda\rho) = I_{2p+1}(\lambda\rho)$$

$$A_x = -\frac{\Gamma}{\pi^2}\left[\cos\theta \int_o^\infty \left\{ \int_c^d K_o(\lambda\beta)d\beta \right\} I_1(\lambda\rho)\sin\xi\lambda d\lambda \right.$$

$$+ \sum_{p=1}^{\infty} \cos(2p-1)\theta \int_o^\infty \left\{ \int_c^d K_{2p}(\lambda\beta)d\beta \right\} I_{2p-1}(\lambda\rho)\sin\xi\lambda d\lambda$$

$$\left. + \sum_{p=1}^{\infty} \cos(2p+1)\theta \int_o^\infty \left\{ \int_c^d K_{2p}(\lambda\beta)d\beta \right\} I_{2p+1}(\lambda\rho)\sin\xi\lambda d\lambda \right] + g(\rho,\theta)$$

$$A_x = -\frac{\Gamma}{\pi^2}\left[\cos\theta \int_o^\infty \left\{ \int_c^d K_o(\lambda\beta)d\beta \right\} I_1(\lambda\rho)\sin\xi\lambda d\lambda \right.$$

$$+ \cos\theta \int_o^\infty \left\{ \int_c^d K_2(\lambda\beta)d\beta \right\} I_1(\lambda\rho)\sin\xi\lambda d\lambda$$

$$+ \sum_{p=2}^{\infty} \cos(2p-1)\theta \int_o^\infty \left\{ \int_c^d K_{2p}(\lambda\beta)d\beta \right\} I_{2p-1}(\lambda\rho)\sin\xi\lambda d\lambda$$

$$\left. + \sum_{p=1}^{\infty} \cos(2p+1)\theta \int_o^\infty \left\{ \int_c^d K_{2p}(\lambda\beta)d\beta \right\} I_{2p+1}(\lambda\rho)\sin\xi\lambda d\lambda \right] + g(\rho,\theta)$$

$$A_x = -\frac{\Gamma}{\pi^2}\left[\cos\theta\int_0^\infty\left\{\int_c^d\left[K_o(\lambda\beta)+K_2(\lambda\beta)\right]d\beta\right\}I_1(\lambda\rho)\sin\xi\lambda d\lambda\right.$$

$$\left.+\sum_{p=1}^{\infty}\cos(2p+1)\theta\int_0^\infty\left\{\int_c^d\left[K_{2p}(\lambda\beta)+K_{2p+2}(\lambda\beta)\right]d\beta\right\}I_{2p+1}(\lambda\rho)\sin\xi\lambda d\lambda\right]+g(\rho,\theta)$$

$$A_x = -\frac{\Gamma}{\pi^2}\sum_{p=o}^{\infty}\cos(2p+1)\theta\int_0^\infty\left\{\int_c^d\left[K_{2p}(\lambda\beta)+K_{2p+2}(\lambda\beta)\right]d\beta\right\}I_{2p+1}(\lambda\rho)\sin\xi\lambda d\lambda \tag{28}$$

As before we have put $g(\rho,\theta)=0$, since $g(\rho,\theta)$ is even in ξ, whereas A_x is odd in ξ.

(1) Asymptotic Correlation with Even System

As before, we may verify this expression for A_x by showing that the radial velocity obtained from it at $\xi=\pm\infty$ approaches the correct two-dimensional value. We will consider the general case of a pair of vortices symmetrically spaced with respect to the axis, of span between arbitrary points c and d. We note

$$2K'_{2p+1} = -\left\{K_{2p}+K_{2p+2}\right\}$$

Hence

$$-\int_c^d\left[K_{2p}(\lambda\beta)+K_{2p+2}(\lambda\beta)\right]d\beta = \frac{1}{\lambda}\int_{c\lambda}^{d\lambda}2K'_{2p+1}(\lambda\beta)d(\lambda\beta)$$

$$=\frac{2}{\lambda}K_{2p+1}(\lambda\beta)\Big|_{c\lambda}^{d\lambda}=\frac{2}{\lambda}\left[K_{2p+1}(\lambda d)-K_{2p+1}(\lambda c)\right]$$

We consider first the λd term in the A_x expression:

$$A_{x_d} = \frac{2\Gamma}{\pi^2} \sum_{p=o}^{\infty} \cos(2p+1)\theta \int_o^{\infty} K_{2p+1}(\lambda d)\, I_{2p+1}(\lambda\rho)\, \frac{\sin \xi\lambda}{\lambda}\, d\lambda$$

The radial velocity is obtained from Eq. (11)

$$u_{r_{A_{tr}}} = \frac{1}{r_o \rho} \frac{\partial A_x}{\partial \theta} \tag{11}$$

$$u_{r_{A_{tr}}} = -\frac{2\Gamma}{r_o \rho \pi^2} \sum_{p=o}^{\infty} (2p+1)\sin(2p+1)\theta \int_o^{\infty} K_{2p+1}(\lambda d)\, I_{2p+1}(\lambda\rho)\, \frac{\sin \xi\lambda}{\lambda}\, d\lambda$$

Now consider the limit as $\xi \to \pm \infty$ of the integral

$$J_d = \int_o^{\infty} K_{2p+1}(\lambda d)\, I_{2p+1}(\lambda\rho)\, \frac{\sin \xi\lambda}{\lambda}\, d\lambda$$

Let

$$\xi\lambda = q \qquad d\lambda = \frac{dq}{\xi}$$

$$\lambda = \frac{q}{\xi} \qquad \frac{d\lambda}{\lambda} = \frac{dq}{q}$$

$$\lim_{\xi \to \pm \infty} \int_o^{\infty} K_{2p+1}\left(\frac{qd}{\xi}\right) I_{2p+1}\left(\frac{q\rho}{\xi}\right) \frac{\sin q}{q}\, dq$$

$$= \int_o^{\infty} \frac{1}{2} \frac{(2p+1-1)!}{1} \left(\frac{qd}{2\xi}\right)^{-2p-1} \frac{\left(\frac{1}{2}\frac{q\rho}{\xi}\right)^{2p+1}}{(2p+1)!} \frac{\sin q}{q}\, dq$$

$$= \frac{1}{2} \frac{1}{2p+1} \left(\frac{\rho}{d}\right)^{2p+1} \int_o^{\infty} \frac{\sin q}{q}\, dq$$

Hence

$$J_d = \frac{1}{2} \frac{1}{2p+1} \left(\frac{\rho}{d}\right)^{2p+1} \left(\pm \frac{\pi}{2}\right) \qquad \begin{matrix} + \text{ when } \xi \to + \infty \\ - \text{ when } \xi \to - \infty \end{matrix}$$

And

$$u_{r_{A_{tr_d}}} = \mp \frac{\Gamma}{2r_o\rho\pi} \sum_{p=o}^{\infty} \left(\frac{\rho}{d}\right)^{2p+1} \sin(2p+1)\theta$$

$$= \mp \frac{\Gamma}{2r_o\rho\pi} \sum_{p=o}^{\infty} \frac{\rho^{2p+1}}{d^{2p+1}} \left[\frac{e^{i(2p+1)\theta} - e^{-i(2p+1)\theta}}{2i}\right]$$

Now summing this geometric series in the form x^{2p} :

$$u_{r_{A_{tr_d}}} = \mp \frac{\Gamma}{4\pi r_o \rho\, i} \left[\frac{\frac{\rho}{d} e^{i\theta}}{1 - \frac{\rho^2}{d^2} e^{2i\theta}} - \frac{\frac{\rho}{d} e^{-i\theta}}{1 - \frac{\rho^2}{d^2} e^{-2i\theta}}\right]$$

$$u_{r_{A_{tr_d}}} = \mp \frac{\Gamma d \sin\theta}{2\pi r_o} \left[\frac{d^2 + \rho^2}{d^4 + \rho^4 - 2\rho^2 d^2 \cos 2\theta}\right] \begin{matrix} - \text{ when } \xi \longrightarrow + \infty \\ + \text{ when } \xi \longrightarrow - \infty \end{matrix} \qquad (29)$$

Now if we consider the λc term in the A_x expression, we obtain the same result with d replaced by c, and with the sign reversed. Thus

$$u_{r_{A_{tr_c}}} = \pm \frac{\Gamma c \sin\theta}{2\pi r_o} \left[\frac{c^2 + \rho^2}{c^4 + \rho^4 - 2\rho^2 c^2 \cos 2\theta}\right] \qquad \begin{matrix} + \text{ when } \xi \longrightarrow + \infty \\ - \text{ when } \xi \longrightarrow - \infty \end{matrix} \qquad (29a)$$

The total result is the sum of these two terms.

To check this result, we consider Eq. (20), which was obtained for the case of a vortex inside the jet, as shown in Figure 7.

The two-dimensional derivation of Eq. (20), however, is not restricted in the location of the jet. Hence the same expression will hold when the vortex pair d is outside the jet.

For the vortex pair c , the result is the same with the letter d replaced by c , and with the sign reversed. Thus from two-dimensional theory, we have

$$u_{r_{A_{tr_d}}} = + \frac{\Gamma d \sin\theta}{2\pi r_o} \left[\frac{\rho^2 + d^2}{\rho^4 + d^4 - 2\rho^2 d^2 \cos 2\theta} \right] \tag{20}$$

$$u_{r_{A_{tr_c}}} = - \frac{\Gamma c \sin\theta}{2\pi r_o} \left[\frac{\rho^2 + c^2}{\rho^4 + c^4 - 2\rho^2 c^2 \cos 2\theta} \right] \tag{20a}$$

Hence for a vortex pair outside the jet, the expressions (20) and (20a) are identical with (29) and (29a) which were obtained in the limit as $\xi \longrightarrow \pm \infty$ from the A_x potential of the odd part. The signs are identical when $\xi = -\infty$, which is where the odd part should approach and add to the even part. When $\xi = +\infty$, the signs are opposite, so the odd and even parts cancel, giving the correct representation of no vortex upstream.

This verifies that the expression for A_x given by Eq. (28) is the odd part of strength $\Gamma/2$.

c. Application of Boundary Conditions

(1) Pressure Boundary Condition

The first boundary condition which applies on the surface $\rho = 1$ is:

$$V_j u_j = V_o u_o \tag{1}$$

which on employing Eq. (9) becomes:

$$-V_j\left[-\frac{\sin\theta}{r_o}\frac{\partial A_y}{\partial\rho}-\frac{\cos\theta}{r_o\rho}\frac{\partial A_y}{\partial\theta}+\frac{\partial\phi}{r_o\partial\xi}\right]_j=-V_o\left[-\frac{\sin\theta}{r_o}\frac{\partial A_y}{\partial\rho}-\frac{\cos\theta}{r_o\rho}\frac{\partial A_y}{\partial\theta}+\frac{\partial\phi}{r_o\partial\xi}\right]_o$$

$$\left\{-V_j+V_o\right\}\left[-\frac{\sin\theta}{r_o}\frac{\partial A_y}{\partial\rho}-\frac{\cos\theta}{r_o\rho}\frac{\partial A_y}{\partial\theta}\right]_o-V_j\left[\frac{\partial\phi}{r_o\partial\xi}\right]_j=-V_o\left[\frac{\partial\phi}{r_o\partial\xi}\right]_o$$

On substituting the potentials from Eqs. (27), (6), and (7), and putting $\rho = 1$, we have:

$$\left\{-V_j+V_o\right\}\left[-\frac{\sin\theta}{r_o}\frac{\Gamma}{\pi^2}\int_o^\infty\left\{\int_c^d K_o(\lambda\beta)d\beta\right\}\lambda I_o'(\lambda)\cos\xi\lambda d\lambda\right.$$

$$-\frac{\sin\theta}{r_o}\frac{\Gamma}{\pi^2}\cdot 2\sum_{p=1}^{\infty}\cos 2p\theta\int_o^\infty\left\{\int_c^d K_{2p}(\lambda\beta)d\beta\right\}\lambda I_{2p}'(\lambda)\cos\xi\lambda d\lambda$$

$$\left.+\frac{\cos\theta}{r_o}\frac{\Gamma}{\pi^2}\cdot 2\sum_{p=1}^{\infty}(2p)\sin 2p\theta\int_o^\infty\left\{K_{2p}(\lambda\beta)d\beta\right\}I_{2p}(\lambda)\cos\xi\lambda d\lambda\right]$$

$$-V_j\left[\frac{1}{r_o}\frac{2\Gamma}{\pi^2}\sum_{p=o}^{\infty}\sin(2p+1)\theta\int_o^\infty\lambda A_{2p+1}(\lambda)I_{2p+1}(\lambda)\cos\xi\lambda d\lambda\right]$$

$$=-V_o\left[\frac{1}{r_o}\frac{2\Gamma}{\pi^2}\sum_{p=o}^{\infty}\sin(2p+1)\theta\int_o^\infty\lambda B_{2p+1}(\lambda)K_{2p+1}(\lambda)\cos\xi\lambda d\lambda\right]$$

As before we divide through by $-\frac{\Gamma}{\pi^2 r_o}$, take the Fourier cosine transform with respect to ξ, and divide through by λ :

$$\left\{ V_j - V_o \right\} \left[- \sin\theta \left\{ \int_c^d K_o(\lambda\beta) d\beta \right\} I_o' \right.$$

$$- 2 \sum_{p=1}^{\infty} \sin\theta \cos 2p\theta \left\{ \int_c^d K_{2p}(\lambda\beta) d\beta \right\} I_{2p}'$$

$$\left. + 2 \sum_{p=1}^{\infty} \cos\theta \sin 2p\theta \left\{ \int_c^d K_{2p}(\lambda\beta) d\beta \right\} \frac{2p}{\lambda} I_{2p} \right]$$

$$+ V_j \left[2 \sum_{p=o}^{\infty} \sin(2p+1)\theta \, A_{2p+1} \, I_{2p+1} \right]$$

$$= V_o \left[2 \sum_{p=o}^{\infty} \sin(2p+1)\theta \, B_{2p+1} \, K_{2p+1} \right]$$

We now simplify the terms in the first square bracket, using:

$$2 \sin\theta \cos 2p\theta = \sin(2p+1)\theta - \sin(2p-1)\theta$$

$$2 \cos\theta \sin 2p\theta = \sin(2p+1)\theta + \sin(2p-1)\theta$$

We obtain: $- \sin\theta \left\{ \int_c^d K_o(\lambda\beta) d\beta \right\} I_o'$

$$+ \sum_{p=1}^{\infty} \left\{ - \sin(2p+1)\theta + \sin(2p-1)\theta \right\} \left\{ \int_c^d K_{2p}(\lambda\beta) d\beta \right\} I_{2p}'$$

$$+ \sum_{p=1}^{\infty} \left\{ \sin(2p+1)\theta + \sin(2p-1)\theta \right\} \left\{ \int_c^d K_{2p}(\lambda\beta) \, d\beta \right\} \frac{2p}{\lambda} \, I_{2p}$$

Next using:

$$I_o' = I_1$$

$$I_{2p}'(\lambda) + \frac{2p}{\lambda} I_{2p}(\lambda) = I_{2p-1}(\lambda)$$

$$I_{2p}'(\lambda) - \frac{2p}{\lambda} I_{2p}(\lambda) = I_{2p+1}(\lambda)$$

we obtain:

$$- \sin\theta \left\{ \int_c^d K_o(\lambda\beta)d\beta \right\} I_1$$
$$+ \sum_{p=1}^{\infty} \sin(2p-1)\theta \left\{ \int_c^d K_{2p}(\lambda\beta)d\beta \right\} I_{2p-1}$$
$$- \sum_{p=1}^{\infty} \sin(2p+1)\theta \left\{ \int_c^d K_{2p}(\lambda\beta)d\beta \right\} I_{2p+1}$$

Then:

$$- \sin\theta \left\{ \int_c^d K_o(\lambda\beta)d\beta \right\} I_1 + \sin\theta \left\{ \int_c^d K_2(\lambda\beta)d\beta \right\} I_1$$
$$+ \sum_{p=2}^{\infty} \sin(2p-1)\theta \left\{ \int_c^d K_{2p}(\lambda\beta)d\beta \right\} I_{2p-1}$$
$$- \sum_{p=1}^{\infty} \sin(2p+1)\theta \left\{ \int_c^d K_{2p}(\lambda\beta)d\beta \right\} I_{2p+1}$$

Then:

$$- \sin\theta \int_c^d \left\{ K_o(\lambda\beta) - K_2(\lambda\beta) \right\} d\beta \, I_1$$
$$+ \sum_{p=1}^{\infty} \sin(2p+1)\theta \left\{ \int_c^d K_{2p+2}(\lambda\beta)d\beta \right\} I_{2p+1}$$
$$- \sum_{p=1}^{\infty} \sin(2p+1)\theta \left\{ \int_c^d K_{2p}(\lambda\beta)d\beta \right\} I_{2p+1}$$

Then:

$$- \sin\theta \left\{ \int_c^d \left[K_o(\lambda\beta) - K_2(\lambda\beta) \right] d\beta \right\} I_1$$

$$- \sum_{p=1}^{\infty} \sin(2p+1)\theta \left\{ \int_c^d \left[K_{2p+2}(\lambda\beta) - K_{2p}(\lambda\beta) \right] d\beta \right\} I_{2p+1}$$

Then:

$$\sum_{p=o}^{\infty} \sin(2p+1)\theta \left\{ \int_c^d \left[K_{2p+2}(\lambda\beta) - K_{2p}(\lambda\beta) \right] d\beta \right\} I_{2p+1}$$

Finally

$$\frac{2}{\lambda} \sum_{p=o}^{\infty} (2p+1) \sin(2p+1)\theta \, I_{2p+1} \int_{c\lambda}^{d\lambda} \frac{K_{2p+1}(\lambda\beta)}{\lambda\beta} d(\lambda\beta)$$

The complete equation then becomes:

$$\left\{ V_j - V_o \right\} \frac{2}{\lambda} \sum_{p=o}^{\infty} (2p+1) \sin(2p+1)\theta \, I_{2p+1} \int_{c\lambda}^{d\lambda} \frac{K_{2p+1}(\lambda\beta)}{\lambda\beta} d(\lambda\beta)$$

$$+ 2V_j \sum_{p=o}^{\infty} \sin(2p+1)\theta \, A_{2p+1} I_{2p+1} = 2V_o \sum_{p=o}^{\infty} \sin(2p+1)\theta \, B_{2p+1} K_{2p+1}$$

Equating coefficients of $\sin(2p+1)\theta$, we have

$$\left\{ V_j - V_o \right\} \frac{2}{\lambda} (2p+1) I \int_{c\lambda}^{d\lambda} \frac{K(\lambda\beta)}{\lambda\beta} d(\lambda\beta) + 2V_j AI = 2V_o BK \qquad (30)$$

(2) Kinematic Boundary Condition

The second boundary condition which applies on the surface $\rho = 1$ is:

$$V_o\, u_{r_j} = V_j\, u_{r_o} \tag{2}$$

which on employing Eq. (12) becomes:

$$-V_o\left[\frac{\sin\theta}{r_o}\frac{\partial A_y}{\partial \xi} + \frac{1}{r_o \rho}\frac{\partial A_x}{\partial \theta} + \frac{\partial \phi}{r_o \partial \rho}\right]_j = -V_j\left[\frac{\sin\theta}{r_o}\frac{\partial A_y}{\partial \xi} + \frac{1}{r_o \rho}\frac{\partial A_x}{\partial \theta} + \frac{\partial \phi}{r_o \partial \rho}\right]_o$$

$$\left\{-V_o + V_j\right\}\left[\frac{\sin\theta}{r_o}\frac{\partial A_y}{\partial \xi} + \frac{1}{r_o \rho}\frac{\partial A_x}{\partial \theta}\right]_o - V_o\left[\frac{\partial \phi}{r_o \partial \rho}\right]_j = -V_j\left[\frac{\partial \phi}{r_o \partial \rho}\right]_o$$

On substituting the potentials from Eqs. (27), (28), (6), and (7), and putting $\rho = 1$, we have:

$$\left\{-V_o + V_j\right\}\left[-\frac{\sin\theta}{r_o}\frac{\Gamma}{\pi^2}\int_o^\infty\left\{\int_c^d K_o(\lambda\beta)d\beta\right\}\lambda I_o(\lambda)\sin\xi\lambda d\lambda\right.$$

$$-\frac{\sin\theta}{r_o}\frac{\Gamma}{\pi^2}\cdot 2\sum_{p=1}^{\infty}\cos 2p\theta\int_o^\infty\left\{\int_c^d K_{2p}(\lambda\beta)d\beta\right\}\lambda I_{2p}(\lambda)\sin\xi\lambda d\lambda$$

$$\left.+\frac{1}{r_o}\frac{\Gamma}{\pi^2}\sum_{p=o}^{\infty}(2p+1)\sin(2p+1)\theta\int_o^\infty\left\{\int_c^d\left[K_{2p}(\lambda\beta)+K_{2p+2}(\lambda\beta)\right]d\beta\right\}I_{2p+1}(\lambda)\sin\xi\lambda d\lambda\right]$$

$$-V_o\left[\frac{1}{r_o}\frac{2\Gamma}{\pi^2}\sum_{p=o}^{\infty}\sin(2p+1)\theta\int_o^\infty\lambda A_{2p+1}(\lambda)I'_{2p+1}(\lambda)\sin\xi\lambda d\lambda\right]$$

$$= -V_j\left[\frac{1}{r_o}\frac{2\Gamma}{\pi^2}\sum_{p=o}^{\infty}\sin(2p+1)\theta\int_o^\infty\lambda B_{2p+1}(\lambda)K'_{2p+1}(\lambda)\sin\xi\lambda d\lambda\right]$$

Again we divide through by $-\frac{\Gamma}{\pi^2 r_o}$, take the Fourier sine transform with respect to ξ, and divide through by λ :

$$\left\{V_o - V_j\right\}\left[-\sin\theta\left\{\int_c^d K_o(\lambda\beta)d\beta\right\}I_o\right.$$

$$-2\sum_{p=1}^{\infty}\sin\theta\cos 2p\theta\left\{\int_c^d K_{2p}(\lambda\beta)d\beta\right\}I_{2p}$$

$$\left.+\sum_{p=o}^{\infty}\sin(2p+1)\theta\left\{\int_c^d\left[K_{2p}(\lambda\beta)+K_{2p+2}(\lambda\beta)\right]d\beta\right\}\frac{2p+1}{\lambda}I_{2p+1}\right]$$

$$+V_o\left[2\sum_{p=o}^{\infty}\sin(2p+1)\theta\,A_{2p+1}\,I'_{2p+1}\right]$$

$$=V_j\left[2\sum_{p=o}^{\infty}\sin(2p+1)\theta\,B_{2p+1}\,K'_{2p+1}\right]$$

Simplifying the terms in the first square bracket, using:

$$2\sin\theta\cos 2p\theta=\sin(2p+1)\theta-\sin(2p-1)\theta$$

we obtain:

$$-\sin\theta\left\{\int_c^d K_o(\lambda\beta)d\beta\right\}I_o$$

$$+\sum_{p=1}^{\infty}\left\{-\sin(2p+1)\theta+\sin(2p-1)\theta\right\}\left\{\int_c^d K_{2p}(\lambda\beta)d\beta\right\}I_{2p}$$

$$+\sum_{p=o}^{\infty}\sin(2p+1)\theta\left\{\int_c^d\left[K_{2p}(\lambda\beta)+K_{2p+2}(\lambda\beta)\right]d\beta\right\}\frac{2p+1}{\lambda}I_{2p+1}$$

Then: $$- \sin\theta\left\{\int_c^d K_o(\lambda\beta)d\beta\right\} I_o + \sin\theta\left\{\int_c^d K_2(\lambda\beta)d\beta\right\} I_2$$

$$+ \sum_{p=2}^{\infty} \sin(2p-1)\theta\left\{\int_c^d K_{2p}(\lambda\beta)d\beta\right\} I_{2p}$$

$$- \sum_{p=1}^{\infty} \sin(2p+1)\theta\left\{\int_c^d K_{2p}(\lambda\beta)d\beta\right\} I_{2p}$$

$$+ \sum_{p=o}^{\infty} \sin(2p+1)\theta\left\{\int_c^d \left[K_{2p}(\lambda\beta) + K_{2p+2}(\lambda\beta)\right]d\beta\right\}\frac{2p+1}{\lambda} I_{2p+1}$$

Then:

$$- \sin\theta\left\{\int_c^d K_o(\lambda\beta)d\beta\right\} I_o + \sin\theta\left\{\int_c^d K_2(\lambda\beta)d\beta\right\} I_2$$

$$+ \sum_{p=1}^{\infty} \sin(2p+1)\theta\left\{\int_c^d K_{2p+2}(\lambda\beta)d\beta\right\} I_{2p+2}$$

$$- \sum_{p=1}^{\infty} \sin(2p+1)\theta\left\{\int_c^d K_{2p}(\lambda\beta)d\beta\right\} I_{2p}$$

$$+ \sum_{p=o}^{\infty} \sin(2p+1)\theta\left\{\int_c^d \left[K_{2p}(\lambda\beta) + K_{2p+2}(\lambda\beta)\right]d\beta\right\}\frac{2p+1}{\lambda} I_{2p+1}$$

Then:

$$- \sum_{p=o}^{\infty} \sin(2p+1)\theta\left\{\int_c^d K_{2p}(\lambda\beta)d\beta\right\} I_{2p}$$

$$+ \sum_{p=o}^{\infty} \sin(2p+1)\theta\left\{\int_c^d K_{2p+2}(\lambda\beta)d\beta\right\} I_{2p+2}$$

$$+ \sum_{p=o}^{\infty} \sin(2p+1)\theta\left\{\int_c^d \left[K_{2p}(\lambda\beta) + K_{2p+2}(\lambda\beta)\right]d\beta\right\}\frac{2p+1}{\lambda} I_{2p+1}$$

Now using:

$$\frac{2p+1}{\lambda} I_{2p+1}(\lambda) + I_{2p+2}(\lambda) = I'_{2p+1}(\lambda)$$

$$\frac{2p+1}{\lambda} I_{2p+1}(\lambda) - I_{2p}(\lambda) = - I'_{2p+1}(\lambda)$$

we obtain

$$\sum_{p=o}^{\infty} \sin(2p+1)\,\theta \left\{ \int_c^d \left[K_{2p+2}(\lambda\beta) - K_{2p}(\lambda\beta) \right] d\beta \right\} I'_{2p+1}$$

Finally:

$$\frac{2}{\lambda} \sum_{p=o}^{\infty} (2p+1) \sin(2p+1)\,\theta\, I'_{2p+1} \int_{c\lambda}^{d\lambda} \frac{K_{2p+1}(\lambda\beta)}{\lambda\beta}\, d(\lambda\beta)$$

The complete equation then becomes:

$$\left\{ V_o - V_j \right\} \frac{2}{\lambda} \sum_{p=o}^{\infty} (2p+1) \sin(2p+1)\,\theta\, I'_{2p+1} \int_{c\lambda}^{d\lambda} \frac{K_{2p+1}(\lambda\beta)}{\lambda\beta}\, d(\lambda\beta)$$

$$+2V_o \sum_{p=o}^{\infty} \sin(2p+1)\theta\, A_{2p+1}\, I'_{2p+1} = 2V_j \sum_{p=o}^{\infty} \sin(2p+1)\theta\, B_{2p+1}\, K'_{2p+1}$$

Equating coefficients of $\sin(2p+1)\theta$, we have

$$\left\{ V_o - V_j \right\} \frac{2}{\lambda} (2p+1)\, I' \int_{c\lambda}^{d\lambda} \frac{K(\lambda\beta)}{\lambda\beta}\, d(\lambda\beta) + 2V_o AI' = 2V_j BK' \qquad (31)$$

d. Results

We now have two equations for the two unknowns A and B :

$$\left\{ V_j - V_o \right\} \frac{2}{\lambda} (2p+1)\, I \int_{c\lambda}^{d\lambda} \frac{K(\lambda\beta)}{\lambda\beta}\, d(\lambda\beta) + 2V_j AI = 2V_o BK \qquad (30)$$

$$\left\{V_o - V_j\right\}\frac{2}{\lambda}(2p+1)\,I'\int_{c\lambda}^{d\lambda}\frac{K(\lambda\beta)}{\lambda\beta}\,d(\lambda\beta) + 2V_o\,AI' = 2V_j\,BK' \tag{31}$$

Solving for the coefficients A and B , we obtain:

$$A_{2p+1}(\lambda) = \left[\frac{V_o V_j}{\lambda}\,\frac{1}{V_o^2 I'K - V_j^2 IK'} - 1\right]\frac{2p+1}{\lambda}\int_{c\lambda}^{d\lambda}\frac{K(\lambda\beta)}{\lambda\beta}\,d(\lambda\beta) \tag{32}$$

$$B_{2p+1}(\lambda) = \frac{2p+1}{\lambda}\,\frac{\left\{V_j^2 - V_o^2\right\}II'}{V_o^2 I'K - V_j^2\,IK'}\int_{c\lambda}^{d\lambda}\frac{K(\lambda\beta)}{\lambda\beta}\,d(\lambda\beta) \tag{33}$$

Substituting the values of A and B in the expressions for the potentials, Eqs. (6) and (7), for the case of a horseshoe vortex outside a jet, where all Bessel functions are of the $2p+1$ order:

$$\phi_{jo} = \frac{2\Gamma}{\pi^2}\sum_{p=o}^{\infty}(2p+1)\sin(2p+1)\theta\int_o^{\infty}\left[\frac{V_o V_j}{\lambda}\,\frac{1}{V_o^2 I'K - V_j^2 IK'} - 1\right]\frac{I(\lambda\rho)\sin\xi\lambda\,d\lambda}{\lambda}$$

$$\int_{c\lambda}^{d\lambda}\frac{K(\lambda\beta)}{\lambda\beta}d(\lambda\beta) \tag{6b}$$

$$\phi_{oo} = \frac{2\Gamma}{\pi^2}\sum_{p=o}^{\infty}(2p+1)\sin(2p+1)\theta\int_o^{\infty}\frac{\left\{V_j^2 - V_o^2\right\}II'K(\lambda\rho)}{V_o^2 I'K - V_j^2 IK'}\,\frac{\sin\xi\lambda\,d\lambda}{\lambda}$$

$$\int_{c\lambda}^{d\lambda}\frac{K(\lambda\beta)}{\lambda\beta}\,d(\lambda\beta) \tag{7b}$$

C. Summary of Results

1. Even System

The previously derived expressions for the downwash induced by the boundary due to the even system are collected for convenience. The first index refers to the effect region, and the second to the location of the horseshoe vortex.

Vortex inside jet

$$w_{jj_{even}}(\eta) = \frac{V_j^2 - V_o^2}{V_j^2 + V_o^2} \frac{\Gamma}{4\pi r_o} \left[\frac{1}{\frac{1}{d} - \eta} - \frac{1}{\frac{1}{c} - \eta} + \frac{1}{\frac{1}{d} + \eta} - \frac{1}{\frac{1}{c} + \eta} \right] \tag{3}$$

$$w_{oj_{even}}(\eta) = -\frac{(V_j - V_o)^2}{V_j^2 + V_o^2} \frac{\Gamma}{4\pi r_o} \left[\frac{1}{\eta - c} - \frac{1}{\eta - d} + \frac{1}{\eta + d} - \frac{1}{\eta + c} \right] \tag{4}$$

Vortex outside jet

$$w_{jo_{even}}(\eta) = -\frac{(V_j - V_o)^2}{V_j^2 + V_o^2} \frac{\Gamma}{4\pi r_o} \left[\frac{1}{d - \eta} - \frac{1}{c - \eta} + \frac{1}{d + \eta} - \frac{1}{c + \eta} \right] \tag{25}$$

$$w_{oo_{even}}(\eta) = -\frac{V_j^2 - V_o^2}{V_j^2 + V_o^2} \frac{\Gamma}{4\pi r_o} \left[-\frac{1}{\eta - \frac{1}{d}} + \frac{1}{\eta - \frac{1}{c}} - \frac{1}{\eta + \frac{1}{c}} + \frac{1}{\eta + \frac{1}{d}} \right] \tag{26}$$

Now if we put $V_o / V_j = \mu$, where $0 \leq \mu \leq 1$

$$\frac{V_j^2 - V_o^2}{V_j^2 + V_o^2} = \frac{1 - \mu^2}{1 + \mu^2} \tag{34}$$

$$\frac{(V_j - V_o)^2}{V_j^2 + V_o^2} = \frac{\left[\frac{V_j - V_o}{V_j}\right]^2}{\frac{V_j^2 + V_o^2}{V_j^2}} = \frac{(1-\mu)^2}{1+\mu^2} \tag{35}$$

Employing these results, we have for the downwash induced by the boundary due to the even system:

Vortex inside jet

$$w_{jj_{even}}(\eta) = \frac{1-\mu^2}{1+\mu^2}\frac{\Gamma}{4\pi r_o}\left[\frac{1}{\frac{1}{d}-\eta} - \frac{1}{\frac{1}{c}-\eta} + \frac{1}{\frac{1}{d}+\eta} - \frac{1}{\frac{1}{c}+\eta}\right] \tag{3a}$$

$$w_{oj_{even}}(\eta) = -\frac{(1-\mu)^2}{1+\mu^2}\frac{\Gamma}{4\pi r_o}\left[\frac{1}{\eta-c} - \frac{1}{\eta-d} + \frac{1}{\eta+d} - \frac{1}{\eta+c}\right] \tag{4a}$$

Vortex outside jet

$$w_{jo_{even}}(\eta) = -\frac{(1-\mu)^2}{1+\mu^2}\frac{\Gamma}{4\pi r_o}\left[\frac{1}{d-\eta} - \frac{1}{c-\eta} + \frac{1}{d+\eta} - \frac{1}{c+\eta}\right] \tag{25a}$$

$$w_{oo_{even}}(\eta) = -\frac{1-\mu^2}{1+\mu^2}\frac{\Gamma}{4\pi r_o}\left[-\frac{1}{\eta-\frac{1}{d}} + \frac{1}{\eta-\frac{1}{c}} - \frac{1}{\eta+\frac{1}{c}} + \frac{1}{\eta+\frac{1}{d}}\right] \tag{26a}$$

2. Odd System

a. Expressions for Potentials

We may now similarly collect the four expressions for the potentials of the flow induced by the boundary due to the odd system. These are designated by $\phi_{\nu n}$, where the first index refers to the location of the effect point, and the second to the location of the horseshoe vortex. All Bessel functions are of the 2p+1 order, and are of argument λ unless otherwise shown.

Vortex inside jet

$$\phi_{jj}=\frac{2\Gamma}{\pi^2}\sum_{p=o}^{\infty}(2p+1)\sin(2p+1)\theta\int_o^{\infty}\frac{\left\{V_j^2-V_o^2\right\}KK'I(\lambda\rho)}{\overline{W}}\frac{\sin\xi\lambda d\lambda}{\lambda}\int_{c\lambda}^{d\lambda}\frac{I(\lambda\beta)}{\lambda\beta}d(\lambda\beta) \tag{6a}$$

$$\phi_{oj}=\frac{2\Gamma}{\pi^2}\sum_{p=o}^{\infty}(2p+1)\sin(2p+1)\theta\int_o^{\infty}\left[\frac{V_oV_j}{\lambda\overline{W}}-1\right]\frac{K(\lambda\rho)\sin\xi\lambda d\lambda}{\lambda}\int_{c\lambda}^{d\lambda}\frac{I(\lambda\beta)}{\lambda\beta}d(\lambda\beta) \tag{7a}$$

Vortex outside jet

$$\phi_{jo}=\frac{2\Gamma}{\pi^2}\sum_{p=o}^{\infty}(2p+1)\sin(2p+1)\theta\int_o^{\infty}\left[\frac{V_oV_j}{\lambda\overline{W}}-1\right]\frac{I(\lambda\rho)\sin\xi\lambda d\lambda}{\lambda}\int_{c\lambda}^{d\lambda}\frac{K(\lambda\beta)}{\lambda\beta}d(\lambda\beta) \tag{6b}$$

$$\phi_{oo}=\frac{2\Gamma}{\pi^2}\sum_{p=o}^{\infty}(2p+1)\sin(2p+1)\theta\int_o^{\infty}\frac{\left\{V_j^2-V_o^2\right\}II'K(\lambda\rho)}{\overline{W}}\frac{\sin\xi\lambda d\lambda}{\lambda}\int_{c\lambda}^{d\lambda}\frac{K(\lambda\beta)}{\lambda\beta}d(\lambda\beta) \tag{7b}$$

where $\overline{W}_{2p+1}(\lambda) = V_o^2 I'K - V_j^2 IK'$ (36)

The expression $\overline{W}_{2p+1}$ may be modified as follows:

$$\overline{W} = V_o^2 I'K - V_j^2 IK' + V_o^2 IK' - V_o^2 IK'$$

$$= - V_o^2(IK'-I'K) - (V_j^2 - V_o^2) IK'$$

$$\overline{W} = \frac{V_o^2}{\lambda} - \left\{V_j^2 - V_o^2\right\} IK' \tag{36a}$$

Hence if we put $V_o/V_j = \mu$

$$\frac{V_j^2 - V_o^2}{\bar{W}} = \frac{V_j^2 - V_o^2}{\frac{V_o^2}{\lambda} - \left\{V_j^2 - V_o^2\right\} IK'}$$

$$= \frac{1}{\frac{V_o^2}{\lambda\left\{V_j^2 - V_o^2\right\}} - IK'}$$

$$\frac{V_j^2 - V_o^2}{\bar{W}} = \frac{1}{\frac{1}{\lambda\left\{\frac{1}{\mu^2} - 1\right\}} - IK'} \qquad (37)$$

Also

$$\frac{V_o V_j}{\lambda \bar{W}} = \frac{V_o V_j}{\lambda} \frac{1}{\frac{V_o^2}{\lambda} - \left\{V_j^2 - V_o^2\right\} IK'}$$

$$= \frac{\mu}{\mu^2 - \lambda\left\{1 - \mu^2\right\} IK'}$$

$$\frac{V_o V_j}{\lambda \bar{W}} = \frac{1}{\mu - \lambda\left\{\frac{1}{\mu} - \mu\right\} IK'} \qquad (38)$$

The downwash due to the jet boundary, at points in the plane of the airfoil, may be obtained for each of the four potentials by taking the derivatives:

$$w_{bdry} = \frac{\partial \phi_{\nu n}}{\partial z} = \pm \frac{\partial \phi_{\nu n}}{r \partial \theta} \qquad \left[\begin{array}{l} + \text{ when } \theta = \quad 0^{o} \\ - \text{ when } \theta = 180^{o} \end{array} \right]$$

The derivative with respect to $r\partial\theta$ of the expression in front of the integrals of $\phi_{\nu n}$, which includes the angular function in each case, is:

$$\frac{2\Gamma}{\pi^2 r} \sum_{p=o}^{\infty} (2p+1)^2 \cos (2p+1)\, \theta$$

In the plane of the wing, which we have approximated as the xy plane, θ assumes only the values of 0 and π. For $\theta = 0$, where $\frac{\partial \phi}{\partial z} = + \frac{\partial \phi}{r \partial \theta}$, $\cos (2p+1)\theta = +1$ for all p, and this expression in front of the $\phi_{\nu n}$ integrals is positive. Similarly for $\theta = \pi$, where $\frac{\partial \phi}{\partial z} = - \frac{\partial \phi}{r \partial \theta}$, $\cos (2p+1)\, \theta = -1$ for all p, and this expression is again positive.

Hence in the plane of the wing, for all p, writing $r = r_o \rho$, and noting that in the plane of the wing $\rho = \eta$, the expression in front of the $\phi_{\nu n}$ integrals becomes:

$$+ \frac{2\Gamma}{\pi^2 r_o \eta} \sum_{p=o}^{\infty} (2p+1)^2 \qquad (39)$$

b. Expressions for Downwash

Employing these results, we obtain the downwash induced by the boundary due to the odd system:

Vortex inside jet

$$w_{jj\ odd}(\xi,\eta)=\frac{2\Gamma}{\pi^2 r_o \eta}\sum_{p=o}^{\infty}(2p+1)^2\int_o^{\infty}\frac{KK'I(\eta\lambda)}{\frac{1}{\lambda\left\{\frac{1}{\mu^2}-1\right\}}-IK'}\frac{\sin\xi\lambda d\lambda}{\lambda}\int_{c\lambda}^{d\lambda}\frac{I(\lambda\beta)}{\lambda\beta}d(\lambda\beta) \tag{6c}$$

$$w_{oj\ odd}(\xi,\eta)=\frac{2\Gamma}{\pi^2 r_o \eta}\sum_{p=o}^{\infty}(2p+1)^2\int_o^{\infty}\left[\frac{1}{\mu-\lambda\left\{\frac{1}{\mu}-\mu\right\}IK'}-1\right]\frac{K(\eta\lambda)\sin\xi\lambda d\lambda}{\lambda}\int_{c\lambda}^{d\lambda}\frac{I(\lambda\beta)}{\lambda\beta}d(\lambda\beta) \tag{7c}$$

Vortex outside jet

$$w_{jo\ odd}(\xi,\eta)=\frac{2\Gamma}{\pi^2 r_o \eta}\sum_{p=o}^{\infty}(2p+1)^2\int_o^{\infty}\left[\frac{1}{\mu-\lambda\left\{\frac{1}{\mu}-\mu\right\}IK'}-1\right]\frac{I(\eta\lambda)\sin\xi\lambda d\lambda}{\lambda}\int_{c\lambda}^{d\lambda}\frac{K(\lambda\beta)}{\lambda\beta}d(\lambda\beta) \tag{6d}$$

$$w_{oo\ odd}(\xi,\eta)=\frac{2\Gamma}{\pi^2 r_o \eta}\sum_{p=o}^{\infty}(2p+1)^2\int_o^{\infty}\frac{II'K(\eta\lambda)}{\frac{1}{\lambda\left\{\frac{1}{\mu^2}-1\right\}}-IK'}\frac{\sin\xi\lambda d\lambda}{\lambda}\int_{c\lambda}^{d\lambda}\frac{K(\lambda\beta)}{\lambda\beta}d(\lambda\beta) \tag{7d}$$

c. Convergence of Integrals

The four downwash expressions for the odd system may be investigated in the limit as the variable of integration $\lambda \longrightarrow \infty$ by use of the asymptotic series for the Bessel functions as follows:

$$\lim_{\lambda\to\infty} I_{w_{jj}} = \lim_{\lambda\to\infty}\frac{1}{\eta}\frac{K_{2p+1}K'_{2p+1}I_{2p+1}(\eta\lambda)}{\frac{1}{\frac{1}{\mu^2}-1}-\lambda I_{2p+1}K'_{2p+1}}\int_{c\lambda}^{d\lambda}\frac{I_{2p+1}(\lambda\beta)}{\lambda\beta}d(\lambda\beta)$$

$$= O\frac{1}{\eta}\ \frac{\left[\sqrt{\frac{\pi}{2\lambda}}\,e^{-\lambda}\right]\left[-\sqrt{\frac{\pi}{2\lambda}}\,e^{-\lambda}\right]\left[\frac{1}{\sqrt{2\pi\eta\lambda}}\,e^{\eta\lambda}\right]}{1-\lambda\left[\frac{1}{\sqrt{2\pi\lambda}}\,e^{\lambda}\right]\left[-\sqrt{\frac{\pi}{2\lambda}}\,e^{-\lambda}\right]}\ \int_{c\lambda}^{d\lambda}\frac{e^{\lambda\beta}}{\sqrt{2\pi\lambda\beta}\ \lambda\beta}\,d(\lambda\beta)$$

$$= O\frac{1}{\eta}\ \frac{1}{\lambda}\,e^{-2\lambda}\ \ \frac{1}{\sqrt{\eta\lambda}}\ e^{\eta\lambda}\ \int_{c\lambda}^{d\lambda}\frac{e^{\lambda\beta}}{(\lambda\beta)^{3/2}}\,d(\lambda\beta)$$

Now for this case $\eta \leq 1$. Hence

$$I_{w_{jj}} \leq \frac{e^{(-2+\eta)\lambda}}{\lambda^{3/2}}\ \int_{c\lambda}^{d\lambda}\frac{e^{\lambda\beta}}{(\lambda\beta)^{3/2}}\,d(\lambda\beta)$$

However, since $0 < c \leq \beta \leq d \leq 1$

$$\int_{c\lambda}^{d\lambda}\frac{e^{\lambda\beta}}{(\lambda\beta)^{3/2}}\,d(\lambda\beta) = \int_{c\lambda}^{d\lambda}\frac{e^{t}}{t^{3/2}}\,dt < \frac{1}{(c\lambda)^{3/2}}\int_{c\lambda}^{d\lambda} e^{t}\,dt$$

$$= \frac{1}{(c\lambda)^{3/2}}\left[e^{d\lambda} - e^{c\lambda}\right] < \left(\frac{1}{c}\right)^{3/2}\frac{e^{d\lambda}}{\lambda^{3/2}}$$

Hence: $$I_{w_{jj}} \leq \frac{e^{(-2+\eta+d)\lambda}}{\lambda^{3}} \leq \frac{1}{\lambda^{3}} \qquad (40)$$

Thus we see that for large λ the integral expression (6c) for w_{jj} will converge at least to the order $\frac{1}{\lambda^3}$ for the case where both the effect point η and the vortex point d are at the jet boundary. The integral will converge exponentially to a stronger degree as either the effect or vortex point is taken farther from the boundary.

The remaining three integrals may be investigated in the limit as $\lambda \longrightarrow \infty$ in a similar manner, and in each case they may be shown to converge with the same rapidity.

3. Asymptotic Correlation of Downwash of Odd and Even Systems

Each of the four expressions for the downwash due to the odd system should in the limit as $\xi \longrightarrow \infty$ approach the corresponding expression for the even system. Considering first the integral of Eq. (6c):

$$I_{w_{jj}odd} = \int_0^\infty \frac{K_{2p+1}K'_{2p+1}I_{2p+1}(\eta\lambda)}{\frac{1}{\lambda\left\{\frac{1}{\mu^2}-1\right\}} - I_{2p+1}K'_{2p+1}} \frac{\sin\xi\lambda\, d\lambda}{\lambda} \int_{c\lambda}^{d\lambda} \frac{I_{2p+1}(\lambda\beta)}{\lambda\beta}\, d(\lambda\beta) \qquad (6c)$$

Now consider the limit as $\xi \longrightarrow \infty$ of this integral.

Let $\xi\lambda = q \qquad d\lambda = \frac{dq}{\xi}$

$\lambda = \frac{q}{\xi} \qquad \frac{d\lambda}{\lambda} = \frac{dq}{q}$

$$\lim_{\xi \to \infty} \int_0^\infty \frac{K_{2p+1}\left(\frac{q}{\xi}\right) K'_{2p+1}\left(\frac{q}{\xi}\right) I_{2p+1}\left(\frac{q\eta}{\xi}\right) \frac{\sin q}{q}\, dq}{\frac{1}{\frac{q}{\xi}\left\{\frac{1}{\mu^2}-1\right\}} - I_{2p+1}\left(\frac{q}{\xi}\right) K'_{2p+1}\left(\frac{q}{\xi}\right)} \int_{c\lambda}^{d\lambda} \frac{I_{2p+1}\left(\frac{q\beta}{\xi}\right)}{\frac{q\beta}{\xi}}\, d\left(\frac{q\beta}{\xi}\right)$$

Substituting the leading term in the expansions around the origin for the Bessel functions leads to:

$$I_{w_{jj_{odd}}} = -\frac{\eta^{2p+1}\left\{d^{2p+1}-c^{2p+1}\right\}}{4(2p+1)^2\left[\frac{\mu^2+1}{2(1-\mu^2)}\right]}\int_0^\infty \frac{\sin q}{q}\,dq$$

$$\therefore I_{w_{jj_{odd}}} = \frac{\eta^{2p+1}}{2(2p+1)^2}\,\frac{1-\mu^2}{1+\mu^2}\left\{c^{2p+1}-d^{2p+1}\right\}\left(\pm\frac{\pi}{2}\right) \quad \begin{matrix} + \text{ when } \xi \longrightarrow \infty \\ - \text{ when } \xi \longrightarrow \infty \end{matrix}$$

Hence:

$$w_{jj_{odd}} = \pm\frac{1-\mu^2}{1+\mu^2}\,\frac{\Gamma}{2\pi r_o \eta}\sum_{p=o}^{\infty}\eta^{2p+1}\left\{c^{2p+1}-d^{2p+1}\right\}$$

Now summing this geometric series in the form x^{2p} :

$$w_{jj_{odd}} = \pm\frac{1-\mu^2}{1+\mu^2}\,\frac{\Gamma}{2\pi r_o \eta}\left[\frac{c\eta}{1-c^2\eta^2}-\frac{d\eta}{1-d^2\eta^2}\right]$$

$$\lim_{\xi\longrightarrow\infty} w_{jj_{odd}}(\xi,\eta) = \pm\frac{1-\mu^2}{1+\mu^2}\,\frac{\Gamma}{4\pi r_o}\left[\frac{1}{\frac{1}{c}-\eta}+\frac{1}{\frac{1}{c}+\eta}-\frac{1}{\frac{1}{d}-\eta}-\frac{1}{\frac{1}{d}+\eta}\right]$$

$$\begin{matrix} + \text{ when } \xi \longrightarrow + \infty \\ - \text{ when } \xi \longrightarrow - \infty \end{matrix} \qquad (41)$$

This Eq. (41) when $\xi \longrightarrow -\infty$ is identical with (3a) for the even part, thus adding to it to represent the complete horseshoe vortex. When $\xi \longrightarrow +\infty$, the signs are opposite, and so cancel

completely.

The remaining three expressions for the downwash due to the odd system may be investigated in the limit as $\xi \longrightarrow \infty$ in a similar manner, and in each case they may be shown to approach the corresponding expression for the even system.

IV. APPLICATION TO AN ARBITRARY WING EXTENDING THROUGH A JET

We have determined a basis for finding the downwash at any point ξ , η in the plane of the wing due to the boundary reaction to a pair of finite horseshoe vortices, symmetrically spaced with respect to the axis of the jet. The total downwash at such a point due to such a pair of horseshoe vortices will then be the sum of this boundary induced downwash and the downwash due to the horseshoe vortices themselves.

The downwash due to a field of finite horseshoe vortices has been conveniently tabulated in several forms (Ref. 15, 16), and so facilitates the calculations of span loadings by finite step methods (Ref. 10). We will therefore compute the boundary induced downwash in a similar manner so that it may be conveniently combined with the referenced tables for the horseshoe vortices to calculate the span loading for an airfoil extending through a jet.

With the total perturbation downwash thus determined over the entire x-y plane, and in particular over the field aft of the lifting line, any wing problem in principle can be solved by lifting surface methods. As an example, we employ the approximate lifting surface method of Weissinger (Ref. 11) as a convenient method of calculating the span loading.

The lifting surface method of Weissinger in effect takes into account the linear variation of downwash along the chord. For such a linear variation, the wing characteristics may be

predicted exactly for infinite aspect ratio by satisfying the boundary condition on the wing surface at the 3/4 chord point. Such a linear variation of downwash is the case for both a flat plate airfoil and a parabolic arc airfoil, and hence would be expected to be a good approximation for most conventional airfoils .

The lifting line approximation assumes no variation of downwash along the chord. Thus the Weissinger lifting surface theory, in taking into account the linear variation of downwash along the chord, is in effect considering the next term in a Taylor's expansion of downwash around the 1/4 chord. If further accuracy were required, say for a more complex cambered airfoil, a second term representing the curvature of the downwash could be employed.

In Ref. 10 and Ref. 16 the wing span is subdivided into a finite number of horseshoe vortices, the spans of which are non-dimensionalized with respect to the wing span. For the jet problem, it is more convenient to non-dimensionalize the lengths with respect to the jet radius. The wing data and the jet data may thus be conveniently combined when the wing span is an integer multiple of the jet radius; for non integer multiples the method may be adjusted at the wing tips to provide suitable data there.

To provide a general and flexible method useful for an arbitrary jet-span combination, we arrange the wing as illustrated in Figure 10 (Ref. 10, Fig. 1, and Ref. 16, Fig. 6). The

wing is replaced by a system of N horseshoe vortices along the quarter-chord line, the spans of which are so chosen that their semi-span s is one-fifth of the jet radius r_o. Thus five such horseshoe vortices are located inside the jet.

Sufficient additional horseshoe vortices of the same semi-span s are placed outside the jet to completely represent the wing span. Thus any arbitrary ratio of jet diameter to wing span arrangement may be represented, simply by employing a sufficient (odd) number of horseshoe vortices to represent the wing span. Ref. 10 includes smaller span vortices at the tips which may be used if a further refinement in accuracy is required.

An equal number of downwash points is taken along the three-quarter chord line, at the midpoint of each elementary horseshoe vortex. The downwash velocity from the total vortex system and the boundary is then equated to the component of local velocity normal to the wing chord at each such downwash point. Application of this tangent flow boundary condition for a symmetrical loading provides a set of $\frac{N+1}{2}$ simultaneous equations in the $\frac{N+1}{2}$ unknown circulation strengths across the span, since the circulation strengths of symmetrical vortex pairs will be identical. Solution of this set of equations provides the span loading.

If the ratio of wing span to the jet diameter is so large as to produce an unwieldy number of simultaneous equations,

the number of horseshoe vortex pairs and hence the number of equations may be reduced by employing larger horseshoe vortex spans outboard where their effect on the jet boundary is less pronounced.

A. Downwash Due to the Wing

The downwash velocity in the plane of a rectangular horseshoe vortex due to the vortex itself is given by the expression

$$w(\tilde{x},\tilde{y}) = \frac{\Gamma}{4\pi} \frac{F(\tilde{x},\tilde{y})}{s} \tag{42}$$

where F is defined in Ref. 10, and the $\tilde{x}$ and $\tilde{y}$ are expressed in horseshoe semi-spans. The values of $F(\tilde{x},\tilde{y})$ are conveniently tabulated in Refs. 15 and 16.

Distributing an odd number N of horseshoe vortices having N downwash points across the wing span (Figure 10), the downwash velocity at any of the downwash points P_ν resulting from the N horseshoe vortices is

$$w(\tilde{x}_\nu, \tilde{y}_\nu) = \frac{1}{4\pi} \sum_{n=1}^{N} \frac{\Gamma_n}{s} F(\tilde{x}_\nu, \tilde{y}_\nu) \tag{43}$$

where

$$\begin{aligned} \tilde{x}_\nu &= p_\nu - p_n \\ \tilde{y}_\nu &= q_\nu - q_n \end{aligned} \tag{44}$$

and the $\tilde{x}$, $\tilde{y}$, p, q notation, and the ν, n subscript notation, as used in this section, is illustrated in Fig. 11. The ν and n are the effect and vortex points respectively counted from the left wing tip.

Since $b/2 = Ns$, we may write (45)

$$w(\tilde{x}_\nu, \tilde{y}_\nu) = \frac{N}{4\pi} \sum_{n=1}^{N} \frac{\Gamma_n}{b/2} F(\tilde{x}_\nu, \tilde{y}_\nu) \tag{46}$$

For cases of symmetrical loading and geometry, the downwash at any of the downwash points P_ν becomes

$$w(\tilde{x}_\nu, \tilde{y}_\nu) = \frac{N}{4\pi} \sum_{n=1}^{\frac{N+1}{2}}{}' \frac{\Gamma_n}{b/2} F_{\nu n} \tag{47}$$

with the coefficient $F_{\nu n}$ being given in terms of geometrical distances measured in horseshoe semi-spans,

$$F_{\nu n} = F\left[(p_\nu - p_n), (q_\nu - q_n)\right] + F\left[(p_\nu - p_n), (q_\nu + q_n)\right] \tag{48}$$

and the prime on the summation sign indicating that for the $\frac{N+1}{2}$ term, representing the single horseshoe vortex at the center of the wing,

$$F_{\nu \frac{N+1}{2}} = F\left[(p_\nu - p_n), (q_\nu - o)\right] \tag{49}$$

This condition may be applied at each downwash point to provide a set of $\frac{N+1}{2}$ simultaneous equations in the $\frac{N+1}{2}$ unknown circulation strengths from Eq. (47):

$$\left[w(\tilde{x}_\nu, \tilde{y}_\nu) = \frac{N}{4\pi} \sum_{n=1}^{\frac{N+1}{2}}{}' \frac{\Gamma_n}{b/2} F_{\nu n} \right]_{\nu = 1, 2, 3 \cdots \frac{N+1}{2}} \tag{50}$$

B. Downwash Due to the Jet Boundary

The expressions for the downwash due to the boundary have been obtained as follows, where the first subscript refers to the location of the effect region, the second to the location of the real vortex, and the even or odd notation refers to the component of the horseshoe vortex:

Even System		Odd System	
Expression	Equation No.	Expression	Equation No.
w_{jj}	3a	w_{jj}	6c
w_{oj}	4a	w_{oj}	7c
w_{jo}	25a	w_{jo}	6d
w_{oo}	26a	w_{oo}	7d

These expressions are all non-dimensionalized with respect to the jet radius r_o. We may combine this boundary downwash with the horseshoe downwash at any particular point, taking note of the different coordinates of the same point in the two systems, due to their being non-dimensionalized on different lengths, and having different origins.

Furthermore, by employing the relation

$$r_o = 5s \tag{51}$$

we may write the boundary downwash expressions in a form where they may be conveniently combined with wing downwash expressions, i.e.

$$w(\xi, \eta) = \frac{\Gamma}{4\pi} \frac{G(\xi, \eta)}{s} \tag{52}$$

where we write the $G(\xi, \eta)$ as a function of ξ, η to emphasize their being non-dimensionalized with respect to the jet radius r_o. By this relationship we define the boundary downwash coefficient, $G_{\nu n}(\xi, \eta)$ as:

$$G_{\nu n}(\xi, \eta) = \frac{4\pi s}{\Gamma} w_{\nu n}(\xi, \eta) \tag{53}$$

The quantities $G_{\nu n}$ may thus be written in terms of the boundary induced downwash expressions previously derived, with the aid of Eq. (51), as follows:

JET BOUNDARY DOWNWASH COEFFICIENTS

Even System

Vortex inside jet

$$G_{jj_{even}}(\eta) = \frac{1}{5}\,\frac{1-\mu^2}{1+\mu^2}\left[\frac{1}{\frac{1}{d}-\eta} - \frac{1}{\frac{1}{c}-\eta} + \frac{1}{\frac{1}{d}+\eta} - \frac{1}{\frac{1}{c}+\eta}\right] \tag{3b}$$

$$G_{oj_{even}}(\eta) = -\frac{1}{5}\,\frac{(1-\mu)^2}{1+\mu^2}\left[\frac{1}{\eta-c} - \frac{1}{\eta-d} + \frac{1}{\eta+d} - \frac{1}{\eta+c}\right] \tag{4b}$$

Vortex outside jet

$$G_{jo_{even}}(\eta) = -\frac{1}{5}\,\frac{(1-\mu)^2}{1+\mu^2}\left[\frac{1}{d-\eta} - \frac{1}{c-\eta} + \frac{1}{d+\eta} - \frac{1}{c+\eta}\right] \tag{25b}$$

$$G_{oo_{even}}(\eta) = -\frac{1}{5}\,\frac{1-\mu^2}{1+\mu^2}\left[\frac{1}{\eta-\frac{1}{c}} - \frac{1}{\eta-\frac{1}{d}} + \frac{1}{\eta+\frac{1}{d}} - \frac{1}{\eta+\frac{1}{c}}\right] \tag{26b}$$

Note:

$$G_{jo_{even}} = G_{oj_{even}} \tag{54}$$

$$G_{oo_{even}} = -G_{jj_{even}} \tag{55}$$

JET BOUNDARY DOWNWASH COEFFICIENTS

Odd System

Vortex inside jet

$$G_{\substack{jj \\ odd}}(\xi,\eta)=\frac{8}{5\pi\eta}\sum_{p=o}^{\infty}(2p+1)^2\int_o^{\infty}\frac{KK'I(\eta\lambda)\sin\xi\lambda d\lambda}{\frac{1}{\left\{\frac{1}{\mu^2}-1\right\}}-\lambda IK'}\int_{c\lambda}^{d\lambda}\frac{I(\lambda\beta)}{\lambda\beta}\,d(\lambda\beta) \tag{6e}$$

$$G_{\substack{oj \\ odd}}(\xi,\eta)=\frac{8}{5\pi\eta}\sum_{p=o}^{\infty}(2p+1)^2\int_o^{\infty}\left[\frac{1}{\mu-\lambda\left\{\frac{1}{\mu}-\mu\right\}IK'}-1\right]\frac{K(\eta\lambda)\sin\xi\lambda d\lambda}{\lambda}\int_{c\lambda}^{d\lambda}\frac{I(\lambda\beta)}{\lambda\beta}d(\lambda\beta) \tag{7e}$$

Vortex outside jet

$$G_{\substack{jo \\ odd}}(\xi,\eta)=\frac{8}{5\pi\eta}\sum_{p=o}^{\infty}(2p+1)^2\int_o^{\infty}\left[\frac{1}{\mu-\lambda\left\{\frac{1}{\mu}-\mu\right\}IK'}-1\right]\frac{I(\eta\lambda)\sin\xi\lambda d\lambda}{\lambda}\int_{c\lambda}^{d\lambda}\frac{K(\lambda\beta)}{\lambda\beta}d(\lambda\beta) \tag{6f}$$

$$G_{\substack{oo \\ odd}}(\xi,\eta)=\frac{8}{5\pi\eta}\sum_{p=o}^{\infty}(2p+1)^2\int_o^{\infty}\frac{II'K(\eta\lambda)\sin\xi\lambda d\lambda}{\frac{1}{\left\{\frac{1}{\mu 2}-1\right\}}-\lambda IK'}\int_{c\lambda}^{d\lambda}\frac{K(\lambda\beta)}{\lambda\beta}\,d(\lambda\beta) \tag{7f}$$

All Bessel functions are of 2p+1 order, and unless otherwise shown are of argument λ.

These boundary downwash coefficients may be employed in a manner similar to the wing downwash coefficients. Thus for an odd number N of horseshoe vortices having N downwash points across the wing span (Fig. 10), the downwash velocity at any of the downwash points P_ν resulting from the boundary reaction to the N horseshoe vortices is

$$w(\xi_\nu, \eta_\nu) = \frac{1}{4\pi} \sum_{n=1}^{\frac{N+1}{2}}{}' \frac{\Gamma_n}{s} G_{\nu n} \tag{56}$$

for symmetrical loading, the prime on the summation again indicating the unique character of the center horseshoe vortex. Here the $G_{\nu n}$ is the sum of the even and odd parts. As before, this expression may be written:

$$\left[w(\xi_\nu, \eta_\nu) = \frac{N}{4\pi} \sum_{n=1}^{\frac{N+1}{2}}{}' \frac{\Gamma_n}{b/2} G_{\nu n} \right]_{\nu=1, 2, 3 \cdots \frac{N+1}{2}} \tag{57}$$

C. Total Downwash Due to a Wing Jet Combination

For small angles, the tangent-flow boundary condition

$$w(\tilde{x}_\nu, \tilde{y}_\nu) = V_\nu \sin \alpha_\nu \cong V_\nu \alpha_\nu \tag{58}$$

may be applied at each of the downwash points. Thus, combining Eqs. (50) and (57), and using (58), we have as our final set of $\frac{N+1}{2}$ simultaneous equations in the $\frac{N+1}{2}$ unknown circulation strengths:

$$\left[V_\nu \alpha_\nu = w_\nu = \frac{N}{4\pi} \sum_{n=1}^{\frac{N+1}{2}}{}' \frac{\Gamma_n}{b/2} \left\{ F_{\nu n} + G_{\nu n} \right\} \right]_{\nu=1, 2, 3 \cdots \frac{N+1}{2}} \tag{59}$$

This set of equations is written in terms of the wing span b ,

the wing downwash coefficient $F_{\nu n}$ (Ref. 10), and the boundary downwash coefficient $G_{\nu n}$.

The values of F are obtained from Ref. 15. The values of G are computed from the formulas derived in this thesis and presented on pages 70 and 71. Both the even and odd G coefficients must be used in the above equations.

To facilitate the employment of the method derived in this thesis for the determination of characteristics of an arbitrary wing extending through a jet, the G coefficients, both even and odd, have been programmed in a parametric manner for computation by electronic data processing equipment. The required coefficients may thus be readily obtained for any arbitrary wing-jet geometry and for any desired jet velocity ratio.

V. COMPARISON OF THEORY WITH EXPERIMENT

A. General

The present theory provides a means to determine the lift distribution over a wing extending through a circular jet. In order to provide a comparison of the theory with experimental data, measured values of the lift at successive spanwise points must be employed. There is a dearth of such experimental data, particularly at higher values of the jet velocity ratio, where the effect would be expected to be large, and which would accordingly be of interest.

One such set of experiments is that reported by J. Stuper in Ref. 6, employing velocity ratios that are fairly low, yet probably adequate to check the theory. Fig. 16 of Stuper's paper shows the experimental results for a jet velocity ratio $\mu = 0.735$, and for several angles of attack, and also shows the comparison with Koning's theory (Ref. 1).

Stuper employed a rectangular wing 20 by 80 centimeters, thus having a geometric aspect ratio of 4. His use of circular end plates 32 cm in diameter gave his wing an effective aspect ratio of 5.25 (Ref. 8, p. 211). The jet was 12 cm in diameter, so the ratio of jet diameter to wing chord was 0.6, which is thus the aspect ratio of the wing segment immersed in the jet.

Graham (Ref. 5, Fig. 5.5) reproduced the data of Stuper's Fig. 16, and included a comparison with slender body theory. As observed previously, within the jet the experimental data seemed to lie between the two limiting theories, lifting line and slender body. Outside of the jet, neither theory represented the experiments

very well, both lying below the experimental points. Also neither of these theories gave the sharp discontinuity in loading found experimentally at the jet boundary.

B. Method of Computation

In order to provide a comparison of the present theory with Stuper's experiment, the Weissinger application of the theory developed in the previous part of this thesis was employed. The wing-jet geometry reported in Stuper's paper was represented by the arrangement of horseshoe vortices illustrated in Fig. 10.

The segment of the wing in the jet was represented by 5 horseshoe vortices. Stuper's effective aspect ratio of 5.25 gave an effective span of 105 cm. Hence

$$\eta_{tip} = \frac{(b/2)_{effective}}{r_o} = \frac{52.5}{6} \simeq 8.75 \qquad (60)$$

which determined the spanwise extent of the vortex pattern as shown in Fig. 10, thus representing the wing by a total of N = 45 horseshoe vortices.

To use the Weissinger lifting surface method, the downwash due to each of the horseshoe vortices, both from the vortex itself and from the boundary reaction to the vortex, must be determined at the downwash points located at the intersection of the center line of each such elementary horseshoe vortex and the 3/4 chord line of the wing.

The F downwash coefficients, representing the downwash due to the wing itself, are obtained for the vortex pattern of Fig.

11 from the tables of Refs. 15 and 16. In using these tables, the value of the 3/4 chord line must be expressed in terms of the semi-width s of the horseshoe vortex used. On this basis:

$$\tilde{x} = \frac{x}{s} = \frac{-10}{\frac{b/2}{45}} = \frac{-10 \times 45}{52.5} = -8.75 \qquad (61)$$

is the constant value of the 3/4 chord line used in the Stuper experiment.

The required values of the F downwash coefficients at this constant value of $\tilde{x}$ are most conveniently obtained from the tables in Ref. 15. In this table, the distance in the spanwise direction from the line of symmetry of a given horseshoe vortex, expressed in terms of the semi-width s of the horseshoe vortex, is:

$$\tilde{y} = \left| 2 (\nu - n) \right| \qquad (62)$$

The values of the F wing downwash coefficients, for the case $\tilde{x} = -8.75$ used in the Stuper experiment, have been taken from Ref. 15 and are presented in Table 1.

These F downwash coefficients are of the order of unity, and hence were computed in the tables of Ref. 15 to 3 decimal places, in order to provide accuracies of 3 significant figures. Hence the G downwash coefficients, representing the downwash due to the jet boundary, must similarly be computed to 3 decimal places, as the F and G coefficients are to be summed at each downwash point.

The G downwash coefficients may be computed from the

expressions derived in this thesis. In using these expressions, the value of the 3/4 chord line must be expressed in terms of the jet radius r_o used. On this basis:

$$\xi = \frac{x}{r_o} = \frac{-10}{6} = -1\frac{2}{3} \tag{63}$$

is the constant value of the 3/4 chord line used in the Stuper experiment.

The definite integrals in the G_{odd} functions were evaluated by Filon's Simpson's rule, employing electronic data processing equipment. The computing was programmed so that μ, ξ, β, and η were parameters, and in addition the mesh of the variable of integration λ and the upper limit of the integral could be specified. Four values of the summation index p were employed, which included Bessel functions through order seven.

Computations were carried out only for the constant values of $\xi = -1\frac{2}{3}$ and $\mu = 0.735$, corresponding to the experiment of Stuper (Ref. 6). For this case trial runs showed that an interval of $\Delta\lambda = 0.5$, together with an upper limit of λ of about 12 provided sufficiently rapid convergence to give the required accuracy of 3 decimal places, although an upper limit of $\lambda = 25$ was used for the most slowly convergent cases where both the vortex and the effect point were adjacent to the jet boundary.

For the cases where both the effect point and the vortex point were adjacent or close to the jet boundary, the convergence with respect to p was inadequate to give the required accuracy of 3 decimal places for the four values of the summation index p employed. There were eight such cases.

These eight cases were then extended by employing the Aitken ∇^2 process (Ref. 17, p. 126) to improve the rate of convergence of the sequence of partial sums of the series. This process was chosen because it is exact for a geometric series, which the present sums of integrals approach asymptotically for large values of the summation index p.

The four computed terms of the series provide three ratios. The ratios of successive terms monotonically approach a limit, as the order of the Bessel functions approaches infinity, since all integrals monotonically approach a constant times the value of the integrand at $\lambda = 0$ for large p. This limiting ratio is then determined from the initial value of the integrands.

The last two ratios of the computed terms and this limiting ratio were used to fit a hyperbola to provide a fifth term of the series. The Aitken ∇^2 process was then employed three times to provide estimates of the sum of the infinite series. A further ∇^2 extension was made on these three estimates, providing the final accepted value.

The sums thus obtained were bounded by:

(1) an upper bound obtained by taking the last ratio of the computed terms for all terms thereafter, and

(2) a lower bound obtained by taking the limiting ratio as the ratio for all terms after the last computed term.

The computed values of the G jet boundary downwash coefficients, for the case of $\xi = -1\frac{2}{3}$ and $\mu = 0.735$, used in the Stuper experiment, are presented in Table 2. For the eight cases where the G_{odd} coefficients were extended by the Aitken ∇^2 process,

the extended values are those presented in the column, and the partial sums of the first four terms from which the extended values were obtained are shown in adjacent parentheses.

The G coefficients of Table 2 were at this point available for addition to the F coefficients of Table 1 in accordance with Eq. (59), to provide a set of linear simultaneous equations from which the unknown circulation strengths Γ_n could be determined.

It will be recalled that the formulation of the problem leading to Eq. (59) was based on symmetrical loading across the wing span. Hence the circulation of symmetrical vortex pairs was identical. This permitted a reduction of the number of unknown circulation strengths from $N = 45$ to $\frac{N+1}{2} = 23$, the odd number arising from the unique center vortex.

Hence a solution for the symmetrical Stuper wing was obtained by a set of 23 simultaneous equations in the 23 unknown circulation strengths of a half of the wing on one side of the center line. In constructing these equations, the F coefficients for symmetrical vortex pairs were added together.

The G coefficients were derived for symmetrical vortex pairs, and so are already in the proper form for use in the 23 simultaneous equations. However, the G coefficients were computed separately for their even and odd parts, and so the sum of these two parts was used at each downwash point.

The common factors in Eq. (59) may be transposed to the other side of the equation, giving for the Stuper wing outside the

jet, at 12^{o} angle of attack:

$$\frac{4\pi\frac{b}{2}}{N} Va = \frac{4\pi \times 1.722}{45} \times 98.425 \times 0.209 = 9.915 \text{ ft}^2/\text{sec} \tag{64}$$

Inside the jet, where the velocity is increased by a factor of 1.36, this term becomes 13.485 ft^2/sec. Hence Eq. (59), for the case of the Stuper wing at 12^{o} angle of attack, may be written explicitly:

$$\left[\sum_{n=1}^{23}\left\{F_{\nu n} + G_{\nu n_{even}} + G_{\nu n_{odd}}\right\}\Gamma_n = \begin{matrix} 9.915(\nu = 1\text{-}20) \\ 13.485(\nu = 21\text{-}23)\end{matrix}\right]_{\nu=1\text{-}23} \tag{59a}$$

In this equation the $F_{\nu n}$ coefficients are as defined in Eqs. (48) and (49). Table 1 may be used together with Eq. (62) to provide the F coefficients. Table 2 may be used together with Figs. 10 and 11 to provide the G coefficients.

The 23 simultaneous equations with the 23 unknown circulation strengths Γ_n so constructed were solved by an elimination method. The circulation strengths obtained were converted into local lift coefficients, based on V_o, by the expression:

$$c_\ell = \frac{\ell_{\text{local}}}{\frac{1}{2}\rho V_o^2 c} = \frac{\rho(V\Gamma)_{\text{local}}}{\frac{1}{2}\rho V_o^2 c} \tag{65}$$

These local lift coefficients, for the wing and jet combination, were computed as outlined above for the case of an angle of attack of 12^{o}. The local lift coefficients were then linearly reduced

for the angles of 8^{o} and 4^{o}. From these values, for each angle of attack, were subtracted the local lift coefficients of the wing alone. The differences, which are the increase in local lift coefficients due to the jet, were added to the experimental lift coefficients of the wing alone obtained by Stuper (Ref. 6, Fig. 16), and are shown in Fig. 12.

C. Results

The theory of this thesis has been applied to the wing-jet combination investigated experimentally by Stuper in Ref. 6. The correlation, presented in Fig. 12, has been found to be excellent for that portion of the data presented by Stuper which is felt to be valid.

The present theory agrees well with the experimental data of Stuper in the jet, which is the region of greatest effect and hence of principal interest. The strong decrease in the experimental lift observed immediately outside of the jet is explained by Stuper as being due to the friction boundary layer of the fan enclosure.

The large increase in lift obtained experimentally in the region farther from the jet may be explained by the test setup shown by Stuper in his Fig. 20. The jet has a free boundary as it passes over the wing, and a free boundary for a distance of one quarter of the chord upstream from the leading edge. But for about the next two chord lengths upstream the jet has a solid boundary, in the form of the fan enclosure. The present theory, as well as Koning's theory (Ref. 1), is based on the boundary of a free jet, and would not be expected to agree with the results of a solid boundary.

The effect of this solid boundary upstream will reverse the sense of circulation of the image vortices for the upstream region, and similarly reverse the direction of the downwash induced by such image vortices in their representation of the boundary. From the geometry of the wing-jet arrangement, it is seen that the angle subtended by the fan enclosure, and hence the relative effect of the solid boundary, will have a maximum at about six jet radii outboard from the jet center line along the 3/4 chord line. The experimental points of Stuper show such a maximum, as seen from Fig. 12.

Furthermore, the lift increment obtained by the theory is the difference of opposing effects. Examination of these individual effects for the present case of the Stuper experiment has shown the lift increment to be a relatively small difference of large effects. Hence the large effects at appreciable distances from the jet boundary obtained experimentally by Stuper are felt to be understandable in view of the experimental test set-up he employed.

The strong decrease in experimental lift observed immediately outside of the jet could also be partly caused by the solid boundary upstream, although the dynamic pressure drop in the transition region between the jet and the undisturbed flow caused by the friction boundary layer of the fan enclosure would seem to offer an adequate explanation.

The theory of Koning differs from the present theory essentially in that Koning considers only what in this thesis has been termed the even part, and disregards the odd part. Hence the

difference in the results obtained by the present theory must be attributed to the inclusion of the odd part. The several theories are compared in Figure 13, which includes Koning's theory, as computed both by Stuper (Ref. 6, Fig. 16) and by Graham (Ref. 5, Fig. 5.5), as well as slender body theory, as computed by Graham. It is seen that the present theory is in substantial agreement with the valid experimental points in the jet, and lies between lifting line theory and slender body theory, as expected.

As may be observed in Table 2, for the present case of Stuper's experiment the jet boundary downwash coefficients for the odd part were of the same order as those for the even part, particularly for the spanwise points of major contribution near the jet boundary. Hence the agreement of the present theory with the experimental results of Stuper must be attributed to the inclusion of the odd part.

VI. CONCLUSIONS

A strong correlation of the theory with the available experimental data has been demonstrated. The rapid approach of the downwash induced by the jet boundary, caused by the odd parts of horseshoe vortices representing a wing, to its asymptotic even value, downstream of the lifting line, emphasizes the importance of the odd part in obtaining this correlation.

The wing segment immersed in the jet in the Stuper experiment, used for comparison with the theory, was of aspect ratio = 0.6. For this aspect ratio, and for the spanwise points of major contribution near the jet, the boundary induced downwash at the 3/4 chord points used in the Weissinger analysis was almost the Trefftz plane value. The conclusion is clear that for such low aspect ratio immersed segments the use of lifting line theory introduces serious error, and that an approximate lifting surface theory such as that of Weissinger is required.

For wing segments immersed in the jet of aspect ratio of the order of one, the downwash over the wing, and in particular at the 3/4 chord point, will be in general intermediate between the value at the Trefftz plane and half that value at the lifting line. This variation is large, and the lift distribution predicted by the theory is quite sensitive to the value of the downwash used. The present theory provides a means to determine the proper downwash, and more accurate predictions of lift distribution may be obtained thereby.

VII. REFERENCES

1. Koning, C.: "Influence of the Propeller on Other Parts of the Airplane Structure", Aerodynamic Theory, Edited by W. F. Durand, Vol. IV, Berlin (1935).

2. Millikan, C. B.: "The Influence of Running Propellers on Airplane Characteristics", Journal of the Aeronautical Sciences, Vol. 7, No. 3 (1940).

3. Smelt, R. and Davies, H.: "Estimation of Increase in Lift Due to Slipstream", British ARC R and M 1788 (1937).

4. Weil, J. and Sleeman, W. C., Jr.: "Prediction of the Effects of Propeller Operation on the Static Longitudinal Stability of Single-Engine Tractor Monoplanes with Flaps Retracted". NACA TN 1722 (1948).

5. Graham, E. W., Lagerstrom, P. A., Licher, R. M., Beane, B. J.: "A Preliminary Theoretical Investigation of the Effects of Propeller Slipstream on Wing Lift", Douglas Aircraft Co. Report SM-14991 (1953).

6. Stuper, J.: Einfluss des Schraubenstrahls auf Flugel und Leitwerk", Luftfahrtforschung, Vol. 15, No. 4 (1938). Also NACA TM 874 (1938).

7. Lotz, I.: "Korrecktur des Abwindes in Windkanalen mit kreisrunden oder elliptischen Querschnitten", Luftfahrtforschung, Vol. 12, No. 8, (Dec. 25, 1935). p. 250-264. Also NACA TM 801 (1936).

8. von Karman, Th., and Burgers, J. M.: "Influence of Boundaries in the Field of Motion around Airfoil Systems", Aerodynamic

Theory, Edited by W. F. Durand, Vol. II, Berlin (1935).

9. Eisenstadt, Bertram J.: "Boundary Induced Upwash for Yawed and Swept-Back Wings in Closed Circular Wind Tunnels", NACA TN 1265 (1947).

10. Campbell, George S.: "A Finite Step Method for the Calculation of Span Loadings of Unusual Plan Forms", NACA Research Memorandum L50L13 (1951).

11. Weissinger, J.: "Uber die Auftriebsverteilung von Pfeilflugeln", Forschungsbericht Nr 1553 (1942). Also NACA TM 1120 (1947).

12. Gray, A., Mathews, G. B., and MacRobert, T. M.: "A Treatise on Bessel Functions", (1931).

13. Erdelyi, A.: "Higher Transcendental Functions", Vol. 2 (1953).

14. Whittaker, E. T., and Watson, G. N.: "Modern Analysis", (1947).

15. Staff of the Mathematics Division: "Tables of Complete Downwash Due to a Rectangular Vortex", Rep. No. 10754, British A.R.C., July 21, 1947, also published as R and M No. 2461 (1953).

16. Diederich, Franklin W.: "Charts and Tables for Use in Calculations of Downwash of Wings of Arbitrary Plan Form", NACA TN 2353 (1951).

17. Householder, Alston S.: "Principles of Numerical Analysis", (1953).

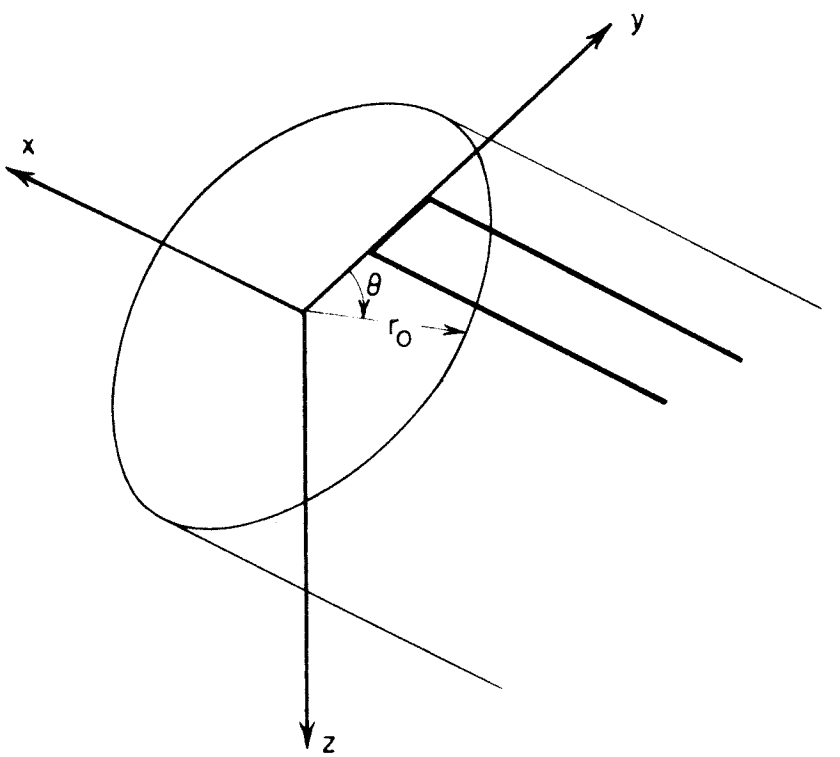

FIG. 1

SYSTEM OF COORDINATES

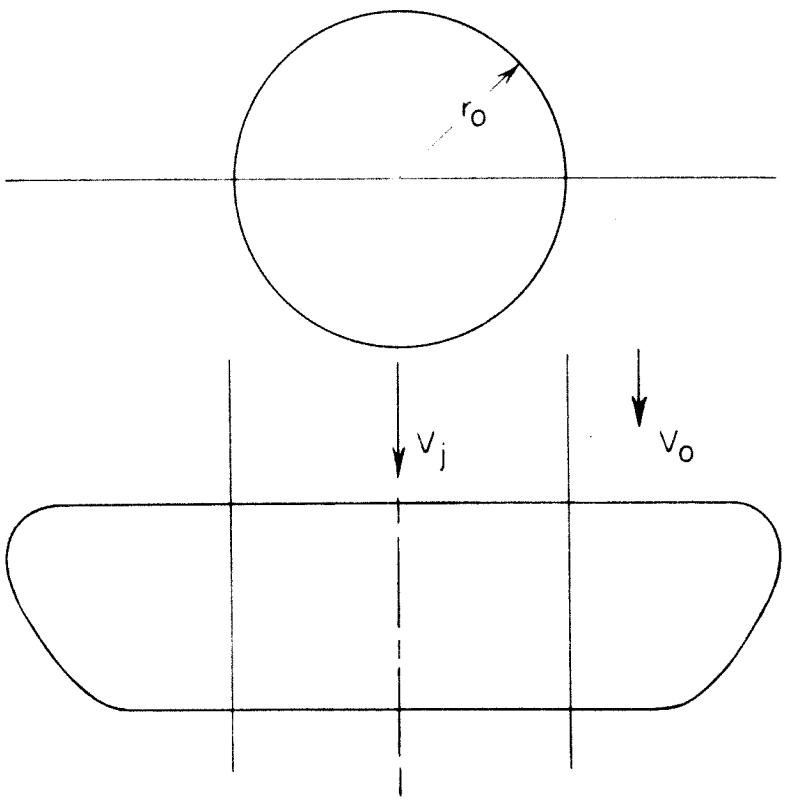

FIG. 2

AIRFOIL SPANNING A CIRCULAR JET

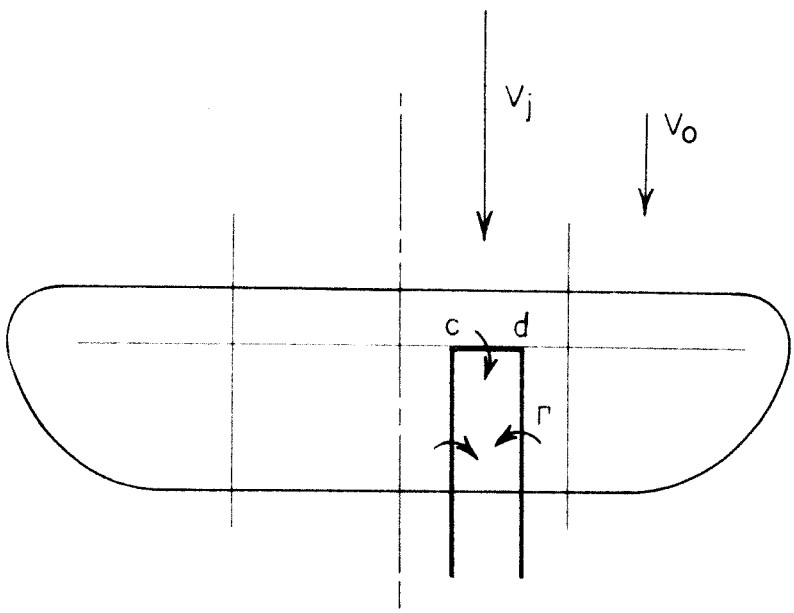

FIG. 3

ELEMENTARY HORSESHOE VORTEX

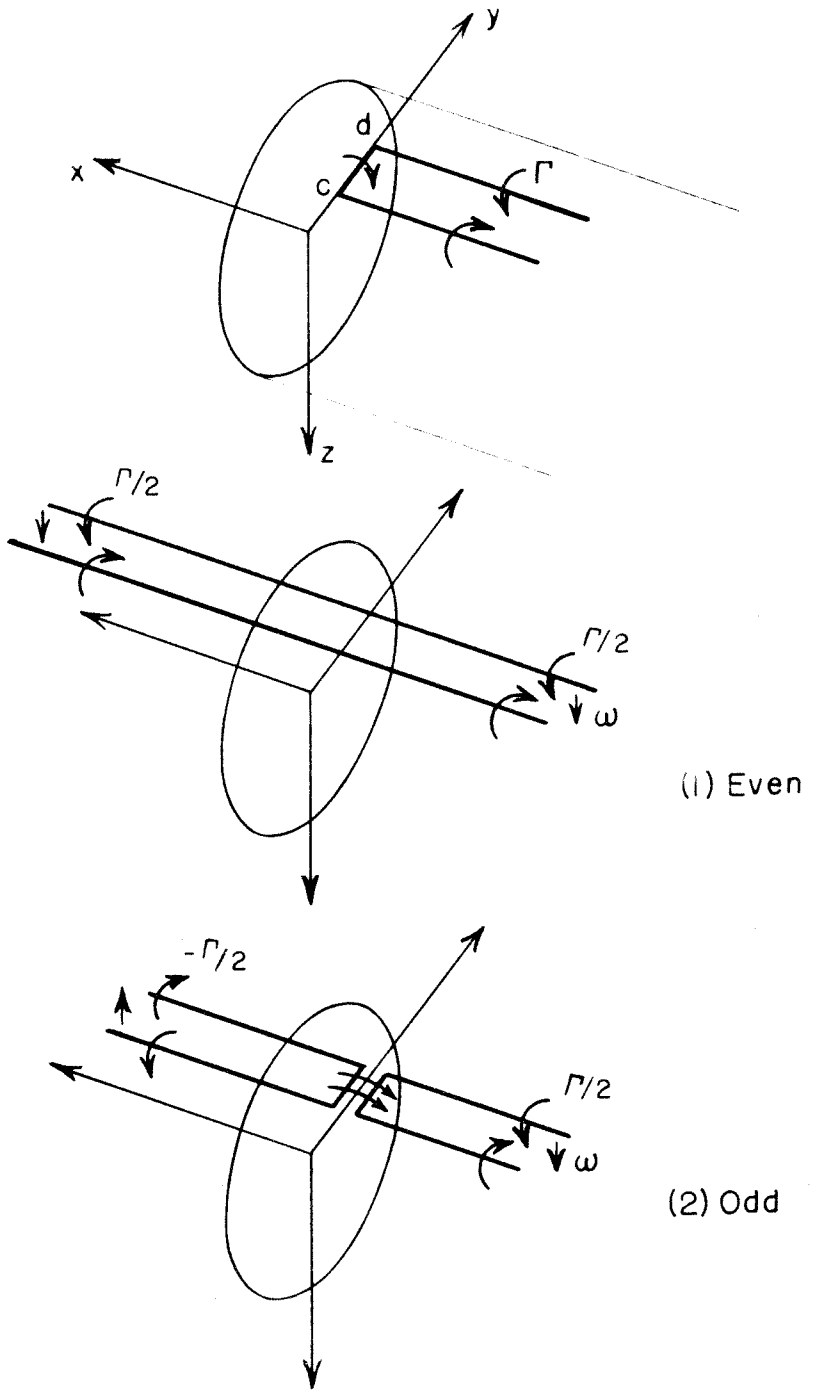

FIG. 4

EVEN AND ODD PARTS OF ELEMENTARY HORSESHOE VORTEX INSIDE JET

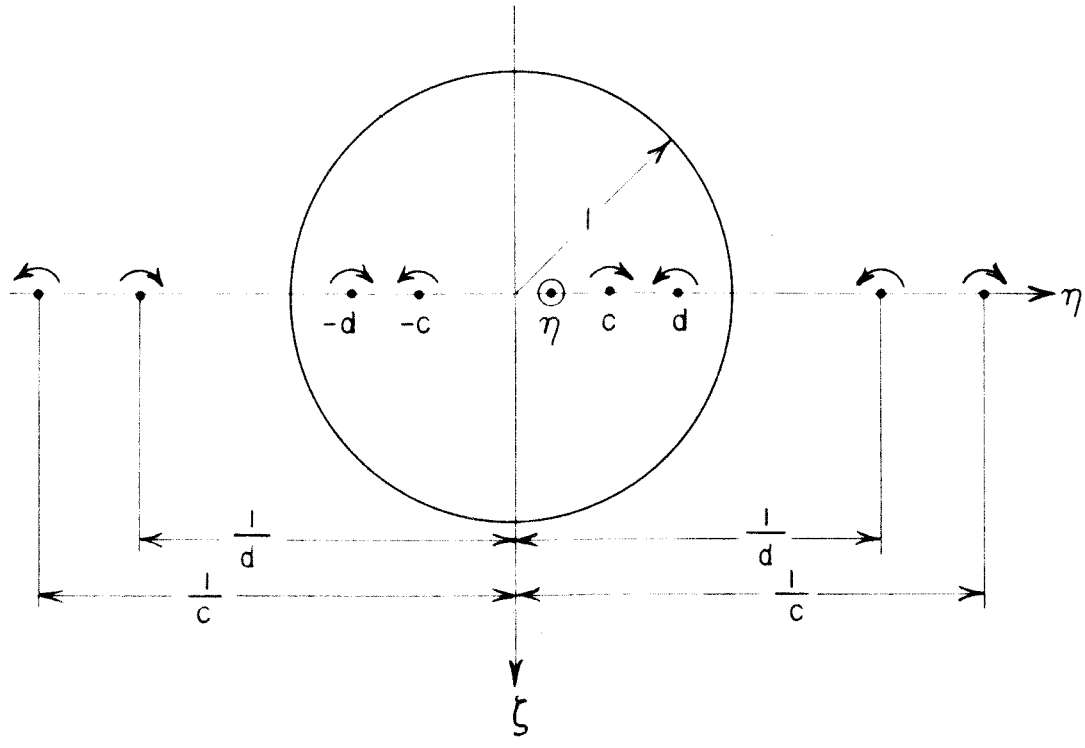

FIG. 5

TWO-DIMENSIONAL VORTEX SYSTEM OF PAIR OF SYMMETRICALLY SPACED HORSESHOE VORTICES INSIDE JET

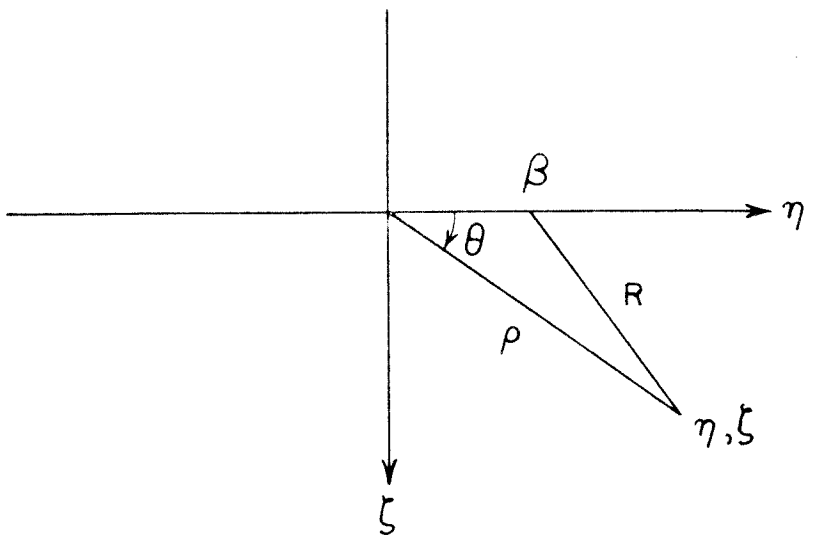

FIG. 6

COSINE LAW GEOMETRY

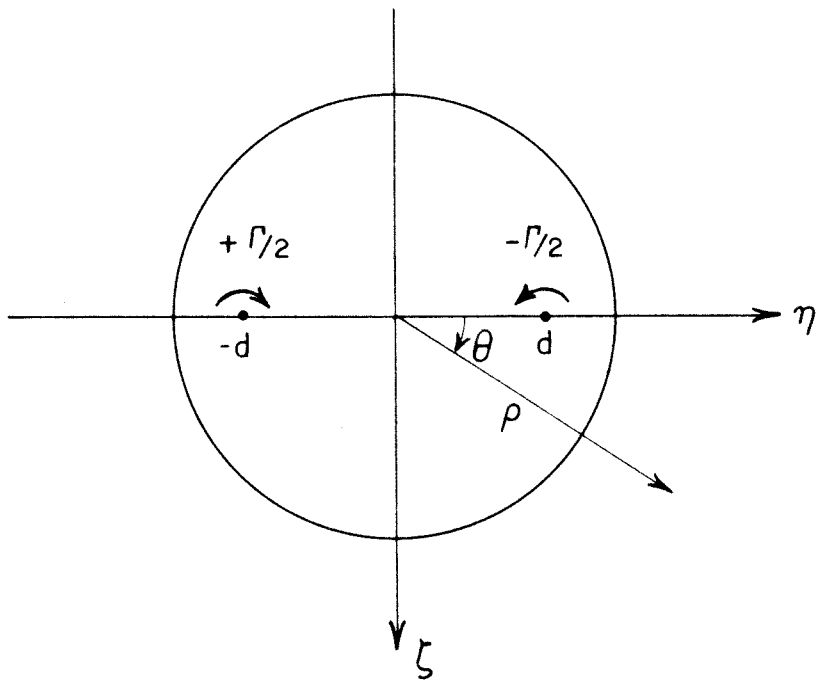

FIG. 7

COMPLEX POTENTIAL GEOMETRY

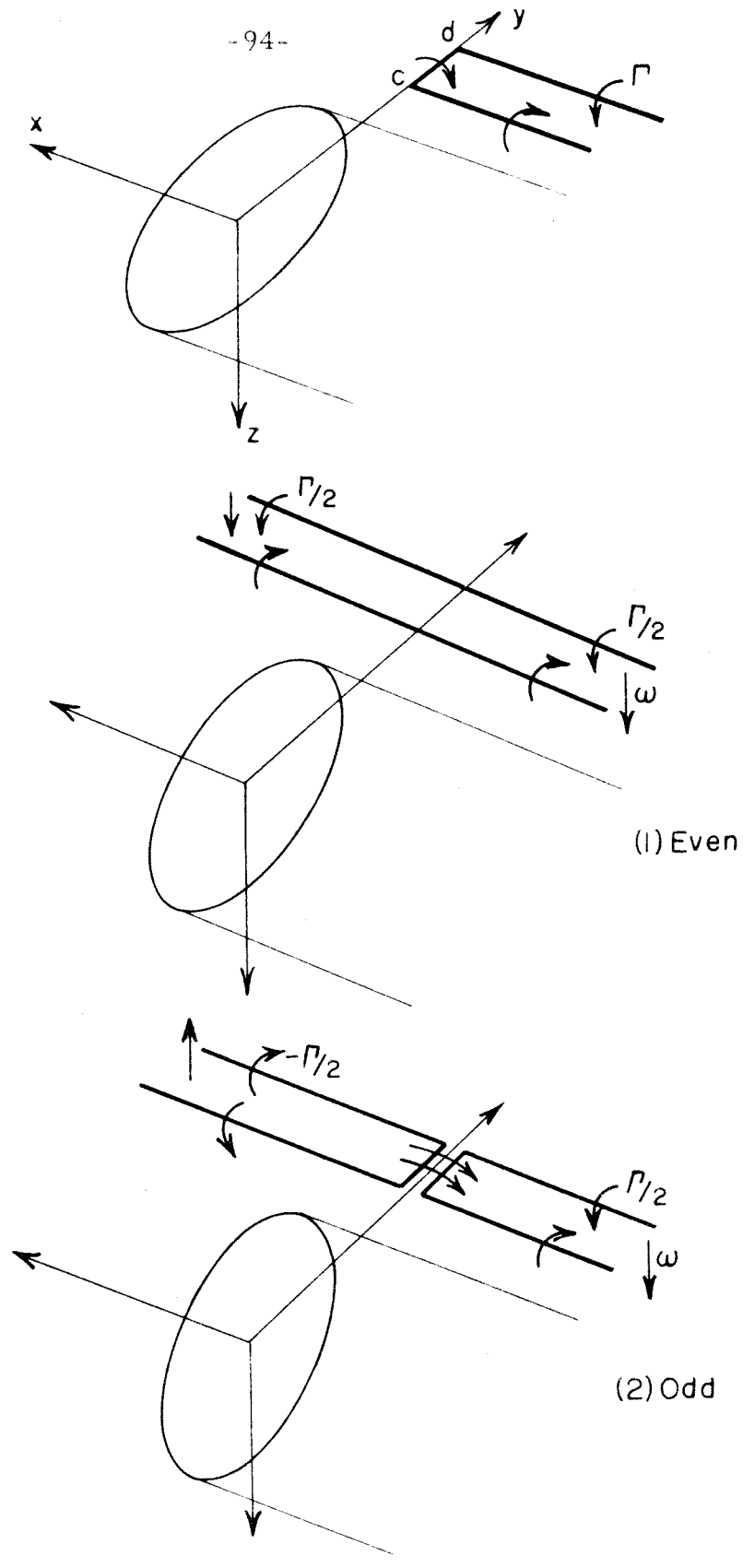

FIG. 8

EVEN AND ODD PARTS OF ELEMENTARY HORSESHOE VORTEX OUTSIDE JET

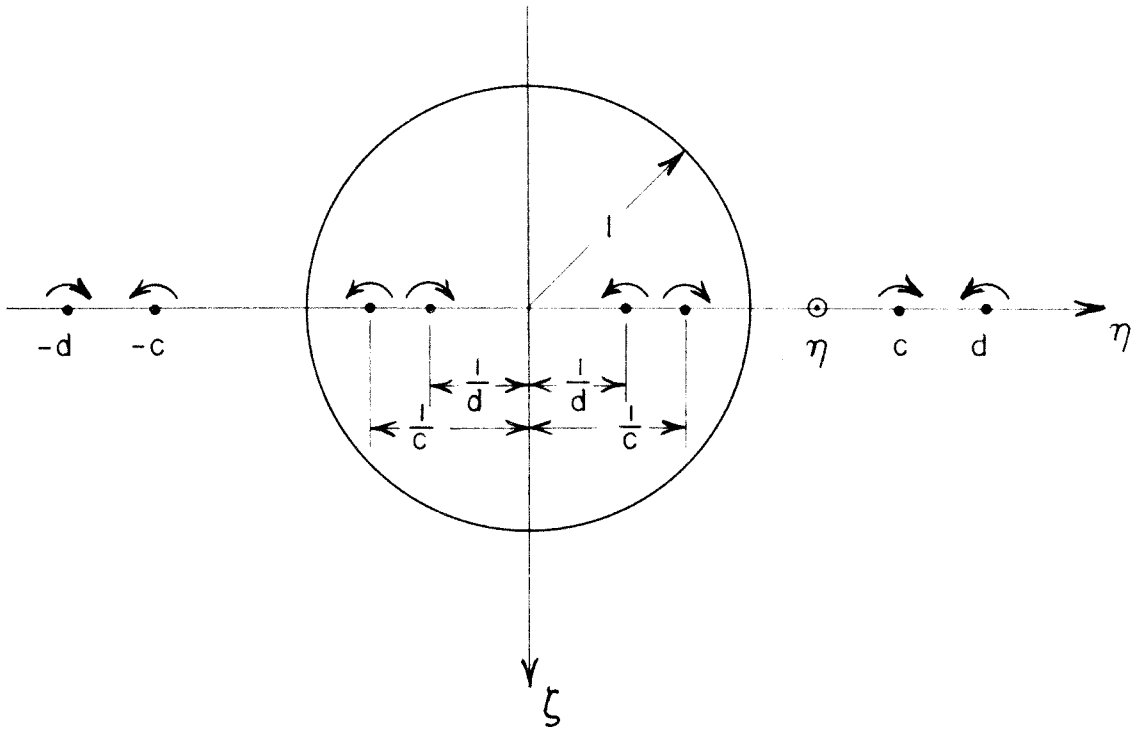

FIG. 9

TWO-DIMENSIONAL VORTEX SYSTEM OF PAIR OF SYMMETRICALLY SPACED HORSESHOE VORTICES OUTSIDE JET

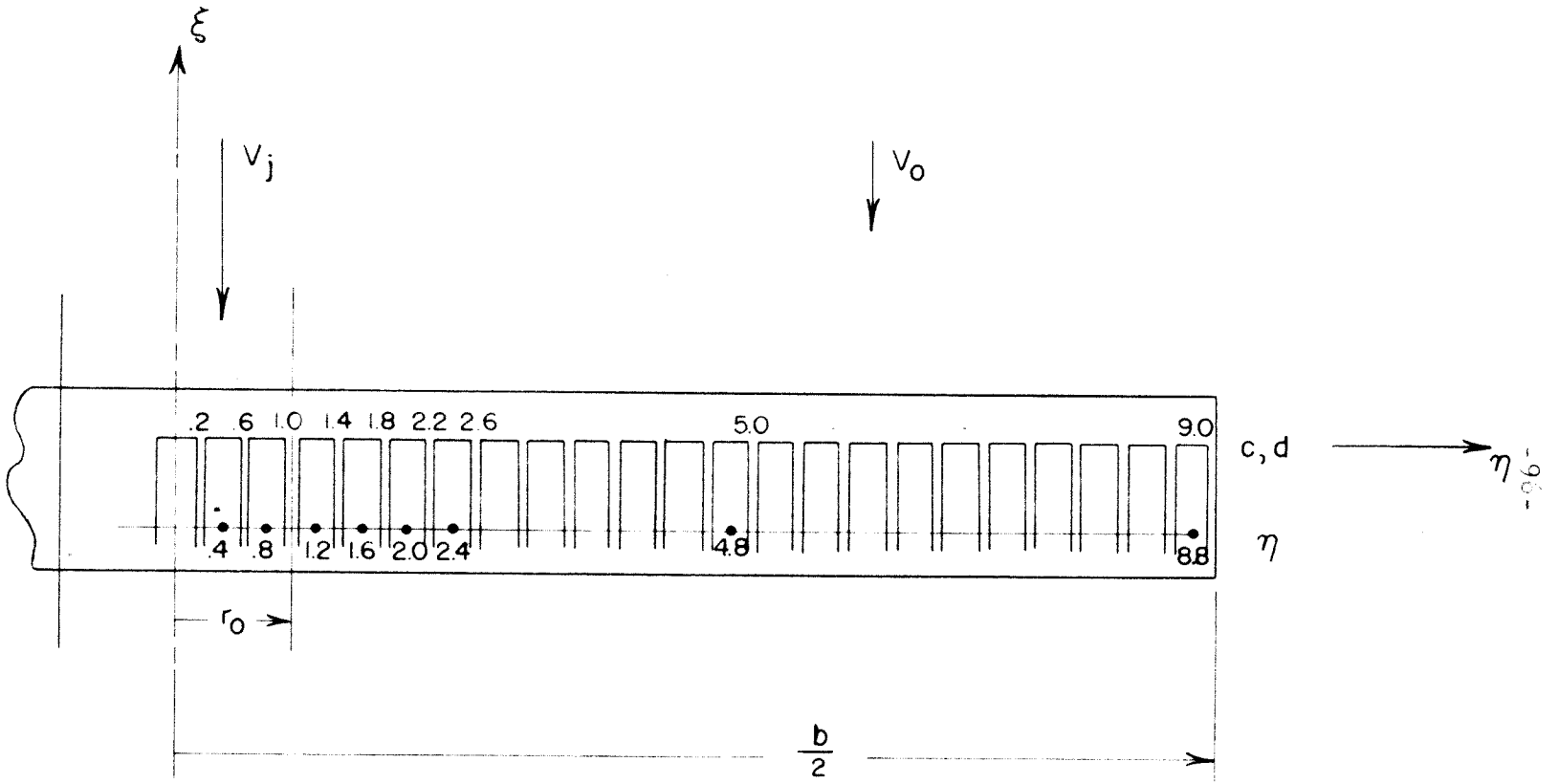

FIG. 10

ARRANGEMENT OF WING-JET VORTEX PATTERN

(WITH NOTATION USED TO DETERMINE JET BOUNDARY DOWNWASH COEFFICIENTS)

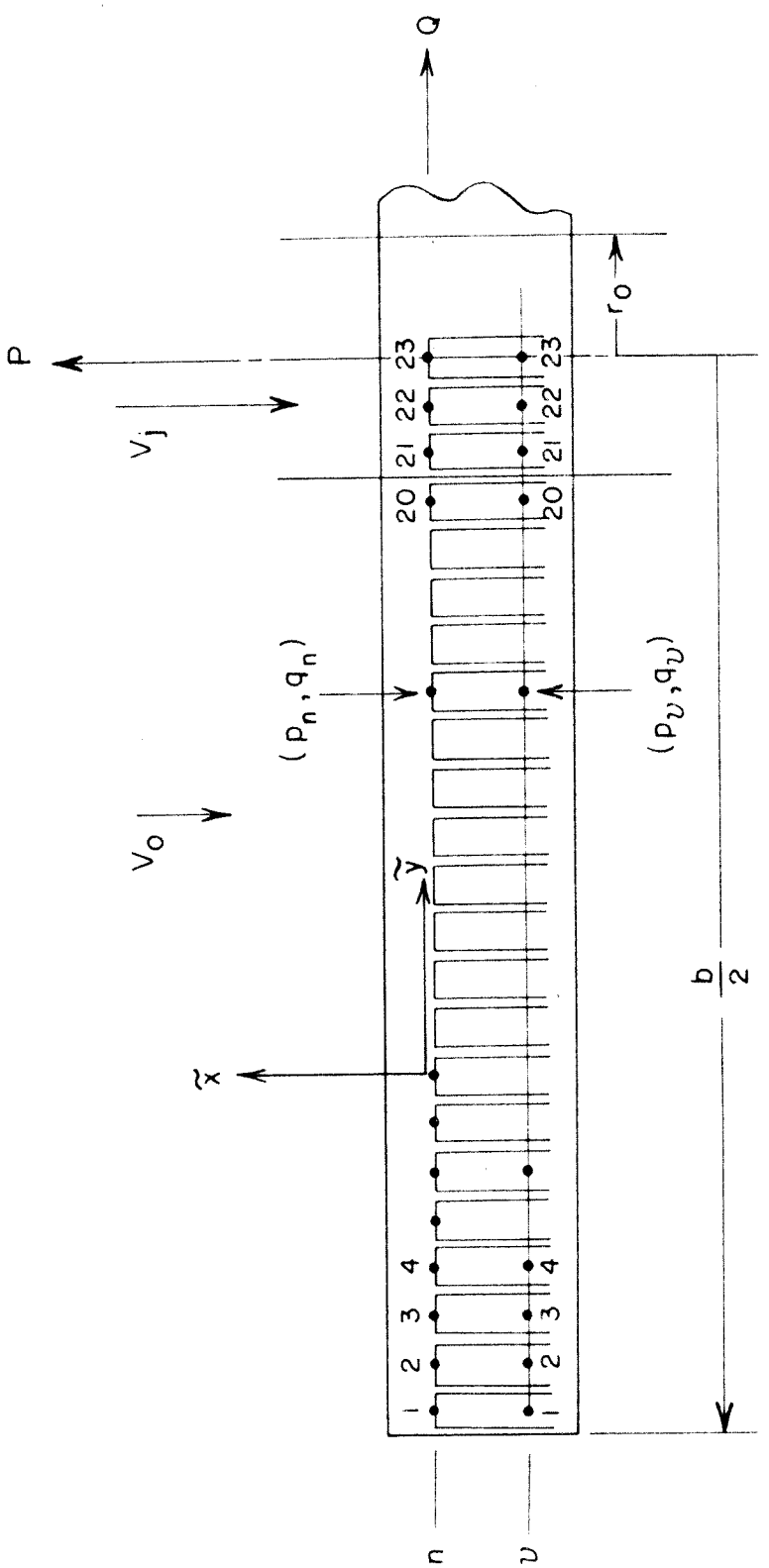

FIG. 11

ARRANGEMENT OF WING-JET VORTEX PATTERN

(WITH NOTATION USED TO DETERMINE LIFT DISTRIBUTION)

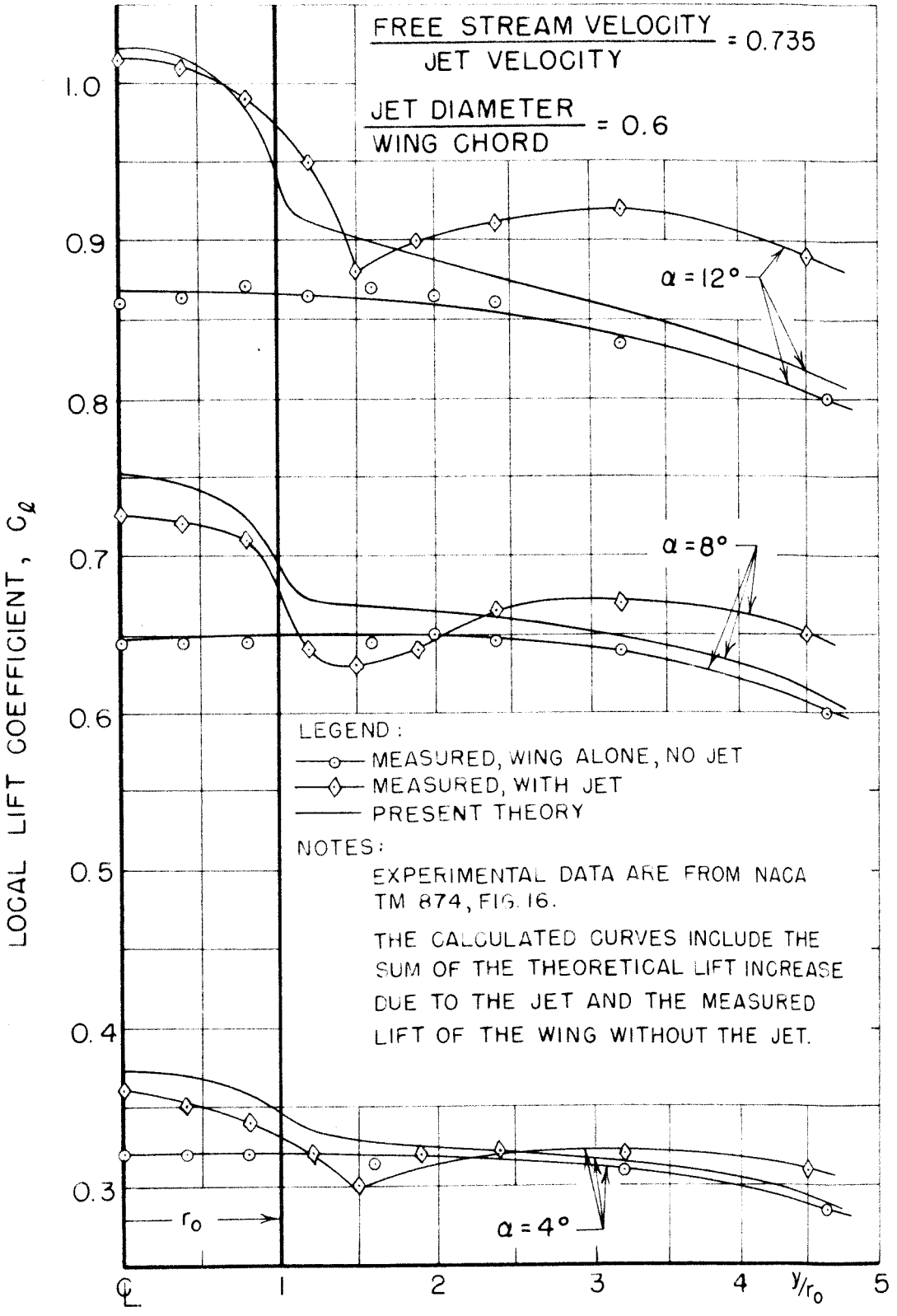

FIG. 12

SPANWISE LIFT DISTRIBUTION ACCORDING TO THEORY AND EXPERIMENT FOR WING EXTENDING THROUGH CIRCULAR JET

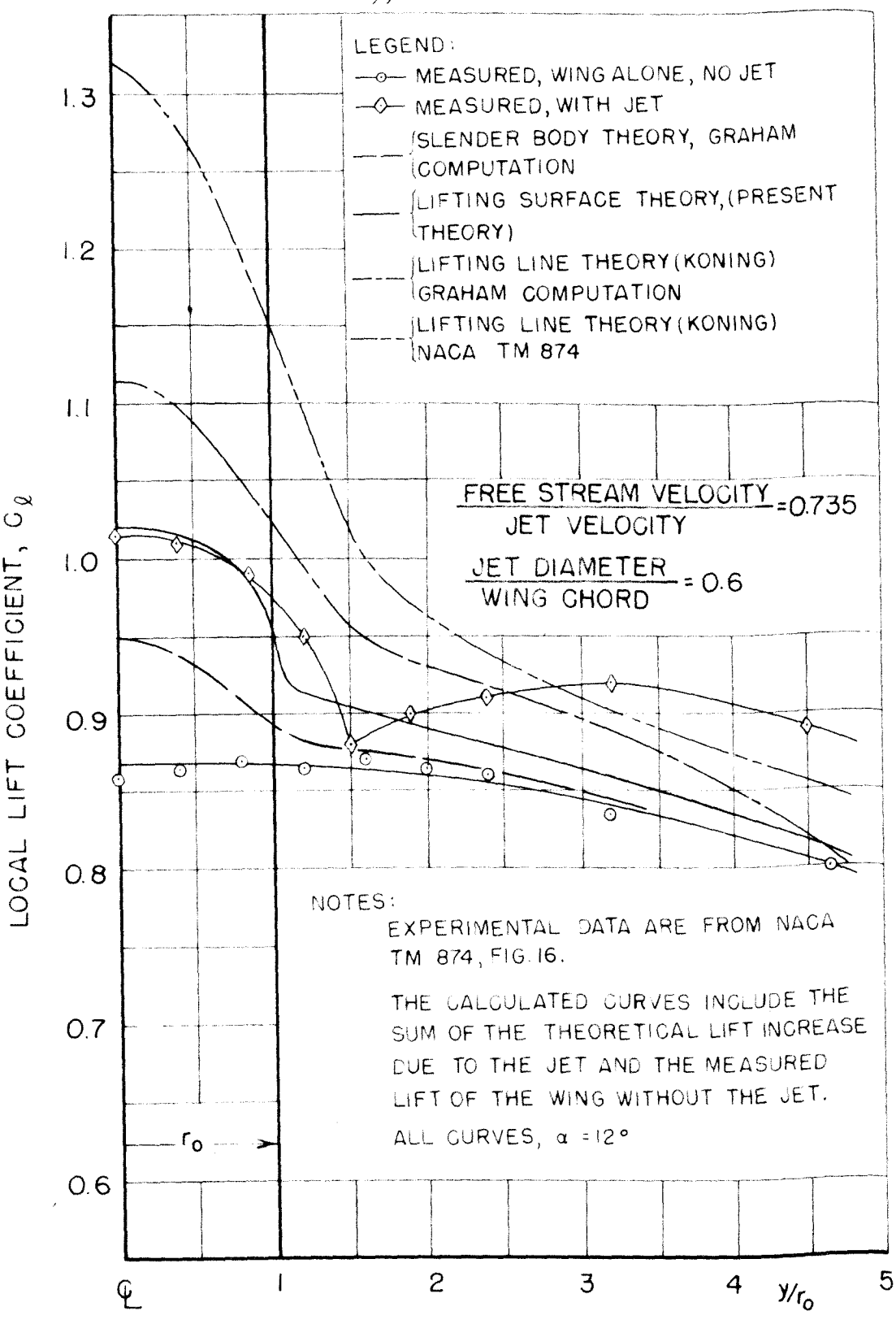

FIG. 13

COMPARISON OF VARIOUS THEORIES WITH EXPERIMENT FOR SPANWISE LIFT DISTRIBUTION OF WING EXTENDING THROUGH CIRCULAR JET

TABLE 1

WING DOWNWASH COEFFICIENTS

($\tilde{x}$ = -8.57)

(Ref. 15)

$\tilde{y}$	F
0	+4.014
2	-1.320
4	-0.255
6	-0.104
8	-0.055
10	-0.033
12	-0.022
14	-0.016
16	-0.012
18	-0.009
20	-0.007
22	-0.006
24	-0.005
26	-0.004
28	-0.003
30	-0.003
32	-0.002
34	-0.002
36	-0.002
38	-0.002
40	-0.002
42	-0.001
44	-0.001
46	-0.001
48	-0.001
50	-0.001
52	-0.001

$\tilde{y}$	F
54	-0.001
56	-0.001
58	-0.001
60	-0.001
62	-0.001
64	-0.001
66	-0.000

TABLE 2

JET BOUNDARY DOWNWASH COEFFICIENTS

($\xi = -1\frac{2}{3}$; $\mu = 0.735$)

η	β	G_{even}	G_{odd}
0	0	0.024*	0.021*
	0.4	0.048	0.042
	0.8	0.048	0.043
	1.2	0.005	0.006
	1.6	0.003	0.003
	2.0	0.002	0.002
	2.4	0.001	0.001
	2.8	0.001	0.001
	3.2	0.001	-
	3.6	0.001	-
0.4	0	0.024*	0.021*
	0.4	0.052	0.047
	0.8	0.066	0.061
	1.2	0.008	0.009
	1.6	0.004	0.004
	2.0	0.002	0.002
	2.4	0.001	0.001
	2.8	0.001	0.001
	3.2	0.001	-
	3.6	0.001	-
0.8	0	0.025*	0.022*
	0.4	0.069	0.064 (0.063)
	0.8	0.239	0.238 (0.179)
	1.2	0.031	0.034 (0.024)
	1.6	0.007	0.007
	2.0	0.003	0.003
	2.4	0.002	0.002

η	β	G_{even}	G_{odd}
0.8	2.8	0.001	0.001
	3.2	0.001	0.001
	3.6	0.001	-
	4.0	0.001	-
1.2	0	0.003*	0.003*
	0.4	0.008	0.009
	0.8	0.031	0.033 (0.023)
	1.2	-0.180	-0.182 (-0.110)
	1.6	-0.033	-0.028 (-0.026)
	2.0	-0.015	-0.011
	2.4	-0.008	-0.005
	2.8	-0.006	-0.003
	3.2	-0.004	-0.002
	3.6	-0.003	-0.001
	4.0	-0.002	-0.001
	4.4	-0.002	-0.001
	4.8	-0.002	-0.001
	5.2	-0.001	-
	5.6	-0.001	-
	6.0	-0.001	-
	6.4	-0.001	-
	6.8	-0.001	-
	7.2	-0.001	-
	7.6	-0.001	-
	8.0	-0.001	-
1.6	0	0.001*	0.002*
	0.4	0.004	0.004
	0.8	0.007	0.007
	1.2	-0.035	-0.030 (-0.028)
	1.6	-0.012	-0.009
	2.0	-0.006	-0.004

η	β	G_{even}	G_{odd}
1.6	2.4	-0.004	-0.002
	2.8	-0.003	-0.001
	3.2	-0.002	-0.001
	3.6	-0.002	-0.001
	4.0	-0.001	-
	4.4	-0.001	-
	4.8	-0.001	-
	5.2	-0.001	-
	5.6	-0.001	-
	6.0	-0.001	-
2.0	0	0.001*	0.001*
	0.4	0.002	0.002
	0.8	0.003	0.003
	1.2	-0.015	-0.011 (-0.011)
	1.6	-0.006	-0.004
	2.0	-0.004	-0.002
	2.4	-0.002	-0.001
	2.8	-0.002	-0.001
	3.2	-0.001	-
	3.6	-0.001	-
	4.0	-0.001	-
	4.4	-0.001	-
	4.8	-0.001	-
2.4	0	0.001*	0.001*
	0.4	0.001	0.001
	0.8	0.002	0.002
	1.2	-0.009	-0.006
	1.6	-0.004	-0.002
	2.0	-0.002	-0.001
	2.4	-0.002	-0.001
	2.8	-0.001	-

η	β	G_{even}	G_{odd}
2.4	3.2	-0.001	-
	3.6	-0.001	-
	4.0	-0.001	-
2.8	0.4	0.001	0.001
	0.8	0.001	0.001
	1.2	-0.006	-0.003
	1.6	-0.003	-0.001
	2.0	-0.002	-0.001
	2.4	-0.001	-
	2.8	-0.001	-
	3.2	-0.001	-
3.2	0.4	0.001	-
	0.8	0.001	0.001
	1.2	-0.004	-0.002
	1.6	-0.002	-0.001
	2.0	-0.001	-
	2.4	-0.001	-
	2.8	-0.001	-
3.6	0.4	0.001	-
	0.8	0.001	-
	1.2	-0.003	-0.001
	1.6	-0.002	-0.001
	2.0	-0.001	-
	2.4	-0.001	-
4.0	0.8	0.001	-
	1.2	-0.002	-0.001
	1.6	-0.001	-
	2.0	-0.001	-
	2.4	-0.001	-

η	β	G_{even}	G_{odd}
4.4	1.2	-0.002	-0.001
	1.6	-0.001	-
	2.0	-0.001	-
4.8	1.2	-0.002	-0.001
	1.6	-0.001	-
	2.0	-0.001	-
5.2	1.2	-0.001	-
	1.6	-0.001	-
5.6	1.2	-0.001	-
	1.6	-0.001	-
6.0	1.2	-0.001	-
	1.6	-0.001	-
6.4	1.2	-0.001	-
6.8	1.2	-0.001	-
7.2	1.2	-0.001	-
7.6	1.2	-0.001	-
8.0	1.2	-0.001	-

*All values are based on a pair of symmetrically spaced horseshoe vortices of span $\Delta\beta = 0.4$, except for the cases $\beta = 0$, where $\Delta\beta = 0.2$. This situation results from the representation of the wing by pairs of symmetrically spaced horseshoe vortices everywhere except at the center of the wing, which is represented by a single unique vortex.